ACCESSIBILITY
Open

OSLO METROPOLITAN UNIVERSITY
STORBYUNIVERSITETET

Master's Degree in
Structural Engineering and Building Technology
Department of Civil Engineering and Energy Technology

MASTER THESIS

THESIS TITLE	DATE
Impact of urban morphology on pressure coefficient on building facades and wind velocity in street canyons - The case of Oslo	15.06.2020
	NUMBER OF PAGES 72/6
AUTHOR(S) Ståle Eiklid Moen	SUPERVISOR(S) Dimitrios Kraniotis

IN COLLABORATION WITH	CONTACT PERSON

SUMMARY

This thesis aims to study how the pressure coefficients and wind velocity will vary within the city of Oslo, with changing urban morphology and aspect ratios. It is common in the modern society to erect high-rise buildings in front of already existing buildings. The study will simulate and investigate how this will impact the wind conditions in the existing urban environment.

3 KEYWORDS
Computational Flud Dynamics
Urban Morphology
Pressure Coefficients

Preface

This Master thesis is a part of a Master of Science in Structural Engineering at Oslo Metropolitan University. I would like to thank my supervisor, Associate Professor Dimitrios Kraniotis (Oslo Met) and Associate Professor Arnab Chaudhuri (Oslo Met) for invaluable guidance and feedback throughout the study.

Oslo Metropolitan University

Oslo, 15-06-2020

Ståle Eiklid Moen

Abstract

This thesis aims to study how the pressure coefficients and wind velocity will vary within the city of Oslo, with changing urban morphology and aspect ratios. It is common in the modern society to erect high-rise buildings in front of already existing buildings. The study will simulate and investigate how this will impact the wind conditions in the existing urban environment. To achieve this simulation, a CFD tool, Star CCM+ has been used. The geometry that have been used in Star CCM+ is originally gathered from Kartverket and is a SOSI file. A workflow of several programs was needed to finally import this SOSI file as a file format compatible with Star CCM+. An area from Barcode and to Løren in Oslo was chosen, as this has several kinds of urban areas, involving high-rise buildings, low-rise buildings, and older high-rise buildings. This geometry is divided in five different regions to fit Star CCM+ restrictions regarding domain size. An important part of this study was to achieve a good mesh solution and apply appropriate physics setting. Pressure coefficients does vary from region to region, Region 1 with high-rise buildings vary more internally in the region than Region 3 where the building mass is lower and much denser. It is also clear that the velocity is dependent on how dense the buildings are located and the aspect ratio of the streets and buildings.

Keywords – Computational Fluid Dynamics, Urban Morphology, Pressure Coefficients

Contents

1 Introduction **1**
1.1 Scope . . . 3
1.2 Objective and research questions . . . 3
1.3 Limitations . . . 3

2 Theory **4**
2.1 Wind . . . 4
2.1.1 Wind loads . . . 5
2.1.2 Wind effects and comfort . . . 6
2.2 Computational Fluid Dynamics . . . 9
2.2.1 Inlet Boundary Conditions . . . 9
2.2.2 Other Boundary Conditions . . . 10
2.2.3 Turbulence models . . . 11

3 Methodology **13**
3.1 Building the 3D model . . . 15
3.2 Star CCM+ . . . 20
3.2.1 Import of geometry . . . 20
3.2.2 Meshing models . . . 23
3.2.3 Boundary Conditions . . . 27
3.2.4 Physics in the model . . . 28

4 Results **29**
4.1 Region 1 . . . 29
4.2 Region 2 . . . 37
4.3 Region 3 . . . 45
4.4 Region 4 . . . 53
4.5 Region 5 . . . 61

5 Discussion **69**
5.1 Pressure coefficients . . . 69
5.2 Wind velocity . . . 70

6 Conclusion **71**

References **72**

Appendix **74**

List of Figures

2.1 Example of pressure coefficients on a building (Jurelionis and Bouris, 2016) 5
2.2 Wind loads on building (Jurelionis and Bouris, 2016) 6
2.3 Boundary conditions in a CFD tool 10
3.1 The flow direction 13
3.2 The wind rose of Oslo, gathered from Meteorologisk Institutt 14
3.3 The workflow from SOSI to .igs 15
3.4 The geometry area as built in Autocad 17
3.5 The geometry with labeled regions 19
3.6 **(a)** Region 1 **(b)** Region 2 **(c)** Region 3 **(d)** Region 4 **(e)** Region 5 . . . 22
3.7 Mesh with problems in details 23
3.8 From mesh in region 1 24
3.9 **(a)** Region 1 **(b)** Region 2 **(c)** Region 3 **(d)** Region 4 **(e)** Region 5 . . . 26
3.10 The boundaries shown in region 1 27
3.11 Enabled physics models 28
4.1 Pressure coefficients in Region 1 29
4.2 Distribution of the Pressure coefficients in Region 1 30
4.3 The location of the sections in Region 1 30
4.4 **(a)** The pressure coefficients in section X1 in Region 1 **(b)** The pressure coefficients in section X2 in Region 1 31
4.5 **(a)** The pressure coefficients in section Y1 in Region 1 **(b)** The pressure coefficients in section Y2 in Region 1 32
4.6 **(a)** The velocity shown in section X1 in Region 1 **(b)** The location of section X1 shown in the first image 33
4.7 **(a)** The velocity shown in section X2 in Region 1 **(b)** The location of section X2 shown in the first image 34
4.8 **(a)** The velocity shown in section Y1 in Region 1 **(b)** The location of section Y1 shown in the first image 35
4.9 **(a)** The velocity shown in section Y2 in Region 1 **(b)** The location of section Y2 shown in the first image 36
4.10 Pressure coefficients in Region 2 37
4.11 Distribution of the Pressure coefficients in Region 2 38
4.12 The location of the sections in Region 2 38
4.13 **(a)** The pressure coefficients in section X1 in Region 2 **(b)** The pressure coefficients in section X2 in Region 2 39
4.14 **(a)** The pressure coefficients in section Y1 in Region 2 **(b)** The pressure coefficients in section Y2 in Region 2 40
4.15 **(a)** The velocity shown in section X1 in Region 2 **(b)** The location of section X1 shown in the first image 41
4.16 **(a)** The velocity shown in section X2 in Region 2 **(b)** The location of section X2 shown in the first image 42
4.17 **(a)** The velocity shown in section Y1 in Region 2 **(b)** The location of section Y1 shown in the first image 43
4.18 **(a)** The velocity shown in section Y2 in Region 2 **(b)** The location of section Y2 shown in the first image 44
4.19 Pressure coefficients in Region 3 45
4.20 Distribution of the Pressure coefficients in Region 3 46

4.21 The location of the sections in Region 3 46
4.22 **(a)** The pressure coefficients from the front line of buildings in Region 3 **(b)** The pressure coefficients in section X1 in Region 3 47
4.23 **(a)** The pressure coefficients in section Y1 in Region 3 **(b)** The pressure coefficients in section Y2 in Region 3 48
4.24 **(a)** The velocity shown in section X1 in Region 3 **(b)** The location of section X1 shown in the first image 49
4.25 **(a)** The velocity shown in section X2 in Region 3 **(b)** The location of section X2 shown in the first image 50
4.26 **(a)** The velocity shown in section Y1 in Region 3 **(b)** The location of section Y1 shown in the first image 51
4.27 **(a)** The velocity shown in section Y2 in Region 3 **(b)** The location of section Y2 shown in the first image 52
4.28 Pressure coefficients in Region 4 53
4.29 Distribution of the Pressure coefficients in Region 4 54
4.30 The location of the sections in Region 4 54
4.31 **(a)** The pressure coefficients in the front line of Region 4 **(b)** The pressure coefficients in section X1 in Region 4 55
4.32 **(a)** The pressure coefficients in section Y1 in Region 4 **(b)** The pressure coefficients in section Y2 in Region 4 56
4.33 **(a)** The velocity shown in section X1 in Region 4 **(b)** The location of section X1 shown in the first image 57
4.34 **(a)** The velocity shown in section X2 in Region 4 **(b)** The location of section X2 shown in the first image 58
4.35 **(a)** The velocity shown in section Y1 in Region 4 **(b)** The location of section Y1 shown in the first image 59
4.36 **(a)** The velocity shown in section Y2 in Region 4 **(b)** The location of section Y2 shown in the first image 60
4.37 Pressure coefficients in Region 5 61
4.38 Distribution of the Pressure coefficients in Region 5 62
4.39 The location of the sections in Region 5 62
4.40 **(a)** The pressure coefficients in the front of Region 5 **(b)** The pressure coefficients in section X1 in Region 5 63
4.41 **(a)** The pressure coefficients in section Y1 in Region 5, flow direction to the left **(b)** The pressure coefficients in section Y1 in Region 5, flow direction to the right 64
4.42 **(a)** The velocity shown in section X1 in Region 5 **(b)** The location of section X1 shown in the first image 65
4.43 **(a)** The velocity shown in section X2 in Region 5 **(b)** The location of section X2 shown in the first image 66
4.44 **(a)** The velocity shown in section Y1 in Region 5 **(b)** The location of section Y1 shown in the first image 67
4.45 **(a)** The velocity shown in section Y2 in Region 5 **(b)** The location of section Y2 shown in the first image 68
A0.1 Residuals region 1 75
A0.2 Residuals region 2 76
A0.3 Residuals region 3 77
A0.4 Residuals region 4 78

A0.5 Residuals region 5 79

List of Tables

2.1 Modified Beaufort scale (Lawson and Penwarden, 1977) 7
2.2 Surface roughness (Abubaker et al., 2018) 9
2.3 Transport equations (Versteeg and Malalasekera, 2007) 11
3.1 Overview of the time spent meshing each region and the total cells in the mesh 27

1 Introduction

Nowadays it is common around the world that the cities are growing larger, and people living in the rural areas of the land are moving to the cities for work. This is a source of several different challenges for the people responsible for planning and execute the expansion of these cities. The challenges can be tied to traffic, housing and climatic environment to name a few. A typical problem for expanding a city is the question of space. The new buildings are more often high-rise buildings to accommodate more people. This is not necessarily the case in all areas within a city, there can be a large difference between different neighbourhoods where some can be mainly low-rise residential buildings and other areas be mainly high-rise buildings. When new tall buildings are built in the outskirt of a city this can change the local environment in an area deeper in the city. Urban planning is important not only for now, but to plan for the future. With the climate changes looming large it is desirable to use the outside environmental factors to the planners benefit. Therefore it is important to know what kind of an impact the urban morphology has on the wind conditions in cities. With the cities getting bigger and more populated it is important to build sustainable neighbourhoods. This way of planning involves research on how wind will affect air infiltration, urban heat islands and the air pollution. The air infiltration can be responsible for a large portion of a buildings energy consumption and this will always be important to keep at a minimum (Jurelionis and Bouris, 2016).

The wind conditions within an urban environment is dependent on different parameters such as the morphology of the buildings in said area. This is called urban morphology and is an important factor for the external air movement in a neighbourhood or an urban area. (Tabrizi et al., 2014) have conducted a simulation regarding the optimal placement of wind turbines on buildings, and in that context discovered that building shape, height, wind direction and roof shape all are factors that influences the air flow around buildings. This together with street cavity ratios also makes an impact on the wind environment within the urban area. In urban morphology there is several important factors such as the geometry of the buildings, topographical features, frontal area density and urban plan area density (Srebric et al., 2015). As previously mentioned these factors will influence

the airflow in and around the building and therefore impact the air-infiltration of the buildings. Within a city there are several different urban areas and they vary with regards to the factors mentioned earlier, the wind will behave differently in a neighbourhood comprised of only low-rise building versus a neighbourhood with high-rise building. In order to simulate these factors, Computational Fluid Dynamics (CFD) is useful as a method of modelling wind flows around any geometry.

As of 2008 half of the population on earth lived in cities, with the number of megacities in the world increased from 3 in 1975 to 19 in 2007 (Parrish and Zhu, 2009). While these megacities (cities with a population of at least 10 million people), is imperative for the worlds economic it is also an enormous source of air pollution (Parrish and Zhu, 2009). The aim of this paper is to research what kind of impact the urban morphology has on the wind environment in the area, and what this does when considering air infiltration and wind loads on building facades. Air infiltration together with urban heat island (UHI) can affect the buildings in the neighbourhood considering the coefficient of performance of heating (COP), ventilation and air conditioning (Jurelionis and Bouris, 2016). High-rise buildings can if not planned and executed correctly lead to high wind speeds at pedestrian level around the buildings (Blocken et al., 2016). The high wind speed will lead to discomfort and in extreme cases dangerous situation, and this shows why it is important to assess the situation regarding wind environment. There are different ways of finding out how the wind conditions are in an urban area, both local measurements and wind tunnel experiments are used and is found to be a good method. However, these methods are time-consuming and expensive when large areas are to be investigated. With this in mind using computational fluid dynamics software is an easier way of getting an overview of the wind conditions in an urban area. CFD-simulations can be a good solution provided the validation of the simulation is good enough.

1.1 Scope

This master thesis aims to relate the urban morphology with pressure coefficients and the velocity magnitude in an urban area within Oslo. To achieve the best possible results it is necessary to divide the research question into three part questions, these are presented in the following subsection.

1.2 Objective and research questions

There will be three part research questions in the thesis. These are presented below;

i) How will pressure coefficients and wind velocity vary in different neighbourhoods within the city of Oslo?
ii) Study and chart the wind conditions and pressure distribution in an urban environment.
iii) Simulate and investigate how newly built high-rise buildings will affect the wind conditions and pressure distribution in an urban environment.

1.3 Limitations

The possibilities and the amount of results available from the simulations of these regions makes it necessary to to determine some limitation, as the the time scope of the master thesis is limited. Five regions will be simulated and there is enough information in the simulated data to study a number of different topics. The only things that will be studied in the simulation results will be the pressure coefficients and the velocity magnitude. In Star CCM+ the turbulence model k-epsilon has been chosen, there are other turbulence models that could be discussed and considered but the decision was that k-epsilon is chosen. In terms of the geometry, initially the idea was to simulate a region ranging from Barcode in Oslo all the way to Disen. This turned out to not be realistic in terms of the time available and the geometry ended up being from Barcode to Løren. When modelling the buildings in the model some general rules were implemented to ease the process. Such as the floor height being set to 3 meters and the general height of an area being set as relatively the same, more on this under the appropriate chapter.

2 Theory

The thesis is about how pressure coefficients and velocity changes in different city regions. In order to study this a CFD tool is used, in this process different topics will be used and discussed. This chapter will present theory related to these topics.

2.1 Wind

Wind is moving air and is important when considering a number of factors in and around buildings. As mentioned wind is air movement relative to the earth, i.e. horizontal winds. Normally when speaking about wind direction, the wind comes from north, south, west or east but it can also blow upward (upwind) or downward (downwind). Typically the wind speeds are highest during the winter time, this is because all wind is dependant on the horizontal differences in temperature, in other words the wind speeds are highest when the difference in temperature between the polar regions and equator are highest (Holmes, 2018). Differences in air pressure is directly the reason for wind, wind blows from high pressure to low pressure and the pressure gradient determines the wind speed. The pressure gradient indicates the pressure drop per unit length (horizontal) (Holmes, 2018).

$$Pressuregradientforce/unitmass = -\frac{1}{\rho_\alpha} * \frac{\partial p}{\partial x} \tag{2.1}$$

The equation above shows the pressure gradient with the ρ_α being the density of air. Holmes (2018) writes that a point in a fluid where there is a pressure gradient, $\partial f/\partial x$, x in a Cartesian coordinate system, that this is resulting a force per unit mass (Holmes, 2018). This is given from equation 2.1.

Wind is a dynamic phenomenon and when the wind working on a surface of for example a building it transforms into a force. These forces that stems from wind is integral to the structural properties of a construction and the pressurization of the wind is also crucial with regards to the indoor air quality of a building. The wind that creates pressure on building facades also creates air flow around the buildings. These air flows can impact the comfort of people venturing out in the street, particularly if the building in question

is a high-rise building. As mentioned, wind in an urban area is dependent on several factors and some of these depends on the local climate. Local climate differs from the macro climate in that it is specified for a smaller area. Macro climate applies to a region and is a benchmark for the local climates within the region. However, the local climates also depend on wind conditions, topography of both the current and the surrounding environment, vegetation, altitude and distance to the water (ocean or lake).

Cóstola et al. (2010) proved that the time-averaged pressure coefficient of wind, Cp is a good indicator on the outdoor environments interaction with air infiltration. The following equation defines the Cp:

$$Cp = \frac{p_x - p_0}{p_d}; p_d = \frac{\rho * U_{ref}^2}{2} \tag{2.2}$$

In equation 2.2 p_x [Pa] represents the static pressure located at any point in the building facade, p_d [Pa] is the dynamic pressure, p_0 [Pa] is the reference static pressure, ρ [kg/m^3] is the density of air and U_{ref} [m/s] is a reference wind speed at a given height. The figure 2.1 shows the air and wind pressure coefficient on a building surface with perpendicular wind.

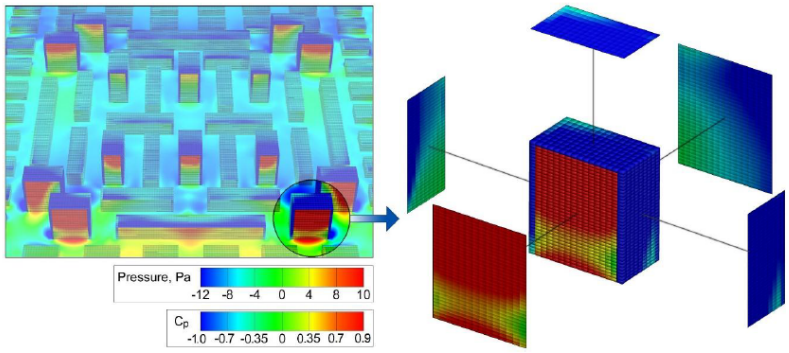

Figure 2.1: Example of pressure coefficients on a building (Jurelionis and Bouris, 2016)

2.1.1 Wind loads

Wind loads together with seismic loads is the dominant environmental loading for structures (Holmes, 2018). Holmes further writes that wind loads has produced roughly the same amount of damage over a long period of time. In 1995, Krishna (1995) wrote that generally all over the world the majority of buildings is reported as categorised low-rise buildings

used for industrial, residential and commercial use, although the trend in the world is that urbanisation causes many high-rise buildings to be built. The low-rise buildings are built in many different types of terrain and topography and the lateral strength of the buildings is governed by wind loads (Krishna, 1995). This is particularly the case with buildings situated in coastal regions or buildings built near or on summits, the exception being settlements in high risk seismic areas.

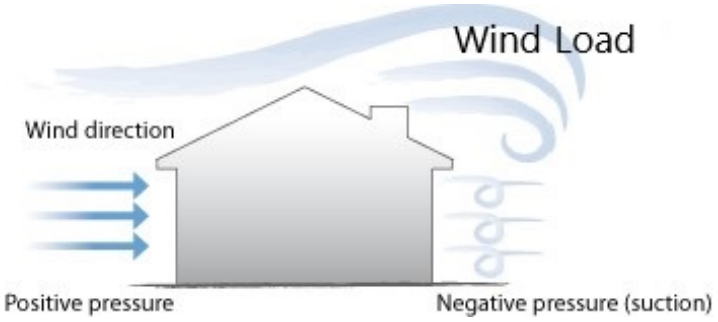

Figure 2.2: Wind loads on building (Jurelionis and Bouris, 2016)

Figure 2.2 shows how the wind typically works on a building. With the positive pressure from the wind on the windward wall and the negative pressure on the leeward wall.

2.1.2 Wind effects and comfort

Wind effects are all the effects that is caused by wind, effects as flapping of clothes, cooling of the body and flying debris and objects (Bottema, 2000). Wind effects are categorized in two blocks; mechanical effects and thermal effects. The mechanical effects directly impacts a person when venturing outside, when a breeze is felt on the body. The thermal effects are much more complex and is dependent on many parameters such as mean wind speed, gust speed, gust duration, air temperature and humidity, clothing and associated moisture content and air permeability, radiation, metabolism and exposure time etc. (Blocken and Carmeliet, 2004). An important factor for the wind environment around buildings is the aspect ratio. This is the ratio of the average building height divided by the width of the streets. Not only does this affect the wind in the area but a denser street will lead to a warmer environment were the heat is blocked in the streets, this can both be an advantage and a disadvantage depending on the climate. Lawson and Penwarden in 1977 provided an extended Beaufort scale that shows the effect of the wind on people (Lawson and Penwarden, 1977). The original Beaufort scale was made in the 1800s by a British

admiral Francis Beaufort and was used to measure the wind when sailing the seas. The modified Beaufort scale by Lawson and Penwarden shows the effects on people rather than sails. The wind speed can be caused by both steady wind and wind gusts (Blocken and Carmeliet, 2004).

Table 2.1: Modified Beaufort scale (Lawson and Penwarden, 1977)

Beaufort Number	Description	Wind Speed at 1.75 m height (m/s)	Effect
0	Calm	0.0–0.1	
1	Light air	0.2–1.0	No noticeable wind
2	Light breeze	1.1–2.3	Wind felt on face
3	Gentle breeze	2.4–3.8	Hair disturbed, clothing flaps, newspaper difficult to read
4	Moderate breeze	3.9–5.5	Raises dust and loose paper, hair disarranged
5	Fresh breeze	5.6–7.5	Force of wind felt on body, danger of stumbling when entering a windy zone
6	Strong breeze	7.6–9.7	Umbrellas used with difficulty, hair blown straight, difficult to walk steadily, sideways wind force about equal to forwards walking force, wind noise on ears unpleasant
7	Near gale	9.8–12.0	Inconvenience felt when walking
8	Gale	12.1–14.5	Generally impedes progress, great difficulty with balance in gusts
9	Strong gale	14.6–17.1	People blown over

Considering the effect wind can have on people it is important to note that wind effect does not equal discomfort. Bottema (Bottema, 2000) defines pedestrian discomfort as follows:

"Pedestrian discomfort occurs when wind effects become so strong, and occur so frequently (say on time scales up to 1 h), that people experiencing those wind effects will start to feel annoyed, and eventually will act in order to avoid these effects".

He and Song (1999) presents that generally two factors impact pedestrian wind comfort, wind speed and frequency. According to them the wind speed directly impacts the comfort of the pedestrian (He and Song, 1999). However, to define when a discomfort sets in it is common to use a wind comfort criterion which is based on a maximum allowed exceedance probability and a discomfort threshold (Blocken and Carmeliet, 2004). This is given by:

$$U_e = U + k * \sigma_u > U_{THR} \tag{2.3}$$

Where U_e is the equivalent wind speed, U is the mean wind speed, k is the peak factor, σ_u represents the standard deviation of the mean speed (turbulence) and U_{THR} is the threshold value of wind speed, all of these parameters is at pedestrian level (Blocken and Carmeliet, 2004). Several studies have dealt with slightly differing parameters. However, most of the discomfort thresholds used is based on the combination of intuition and wind effect rather than actual comfort investigations (Blocken et al., 2016). Wind comfort studies consists of combining statistical meteorological data, aerodynamic information and a comfort criterion. The threshold value does depend heavily on the correlating activity. Wind affects pedestrians differently when taking a stroll around town versus sitting and reading a newspaper at a bench. In there research He and Song (1999) gathered comfort criteria based on different activities and wind speeds. They found that wind speed below 5 m/s has no effect on walking pedestrians while anything above will have an effect (He and Song, 1999). Several studies have considered wind comfort in different cities with different characteristics over the years. Some notable works by Lawson and Penwarden (1977) who analyzed complaints related to wind by shop-owners situated near high-rise buildings. The criterion regarding maximum discomfort probability for walking/strolling found by Lawson and Penwarden (1977) has since been worked on by Bottema (1993) and found to be $P_{max} = 15\%$.

2.2 Computational Fluid Dynamics

Computational fluid dynamics (CFD) is increasingly popular in studies relating to the atomsperic boundary layer, it is a tool that can be used in wide variety within this field (Abubaker et al., 2018).

2.2.1 Inlet Boundary Conditions

Atmospheric boundary layer (ABL) in wind engineering is the part of the atmosphere that is affected by the surface of the earth, this is from the surface of the earth and 200m up in the air. When computing the horizontal wind profile in the atmospheric boundary layer there are two main methods, the logarithmic law (Log law) and the power law.

$$\frac{u}{u_*} = \frac{1}{k} * \ln[\frac{z}{z_0} - \Psi_m(\frac{z}{L}] \tag{2.4}$$

Equation 2.4 is the theory describing interaction between the ground surface and the airflow, it is well known and it originally comes from the work of Monin and Obukhov (Grimenes and Thue-Hansen, 2004). In the above equation u is the velocity at a given height z, k is the von Karman constant which is usually set to 0.4 (Abubaker et al., 2018). u_* is the shear velocity and the z_0 is the surface roughness. The value for the surface roughness can be gathered from table 2.2. Ψ_m is a stability function and can be assumed zero when considering low heights.

Table 2.2: Surface roughness (Abubaker et al., 2018)

Terrain types	roughness length (m)
Very flat terrain (snow, desert)	0.001-0.005
Open terrain (grassland, few trees)	0.01-0.05
Suburban terrain (buildings 3-5 m)	0.1-0.5
Dense urban (buildings 10-30 m)	1-5

The other main method is to use the power law model, the mean wind speed U_z is expressed by the following equation:

$$\frac{U}{U_0} = (\frac{Z}{Z_0})^{\alpha} \tag{2.5}$$

Equation 2.5 is the power law model where the U_0 is the velocity at the height of Z_0, and α is the power law exponent which is determined by the terrain.

2.2.2 Other Boundary Conditions

It is not only the inlet surface that needs to have defined boundary conditions, all the other surfaces including the domain and buildings requires boundary conditions in order to complete the mathematical simulation in a CFD tool. These conditions allow the fluid, in this case air to either enter or to leave the domain. There are several options when choosing the appropriate boundary conditions as shown in figure 2.3:

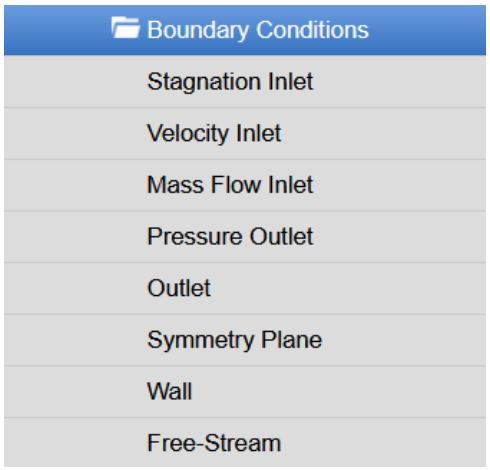

Figure 2.3: Boundary conditions in a CFD tool

In this type of simulation where wind in an urban area is studied it is necessary to have an velocity inlet to allow the fluid to enter the domain, and it is needed to have a outlet in order to show the program where the fluid is leaving, the equation for the face value of the velocity at an outlet boundary condition is shown in the following equation:

$$v = v^{ext} + \frac{x_i}{\rho} * n \tag{2.6}$$

Where the ext means that the value is extrapolated from the adjacent cell, ρ is the density at the boundary face, x_i represents the boundary mass-flux correction factor which is

computed at the outlet boundary.

When considering the walls, roof and floor of the domain several boundary conditions is applicable. The wall condition represent an impermeable surface and is used to confine the fluid, stopping it from leaving the domain (Simcenter, 2020). There are different settings one can apply to the wall to model different kinds of walls, such as no-slip and slip settings. To reduce the extent of the computational domain it is possible to apply the boundary condition symmetry plane, this is used where it is assumed the geometry and flow is symmetric on both sides of the surface. There is no more conditions to specify when applying a symmetry plane. The last boundary condition that is an option of the walls of the domain is free-stream. Simcenter (2020) writes that the free-stream boundary allows the free stream compressible flow conditions at a boundary far away (Simcenter, 2020).

2.2.3 Turbulence models

Versteeg and Malalasekera (2007) writes that in most engineering purposes it is unnecessary to resolve all the details of the fluctuations in turbulence (Versteeg and Malalasekera, 2007). It is sufficient for CFD users to achieve information about time-averaged values of the flow, such as mean pressures, mean velocity and stresses. In order to solve these parameters in CFD it is necessary to use some turbulence models. Reynolds-averaged Navier-Stokes (RANS) equation is a time-averaged equations used to calculate fluid flow motion. To be able to solve the turbulent flow with the RANS equations it is necessary to apply and use a turbulence model (Versteeg and Malalasekera, 2007). The most common RANS turbulence models are categorized on the basis of "number of extra transport equations", as shown in 2.3. These transport equations needs to be solved alongside the flow equations.

Table 2.3: Transport equations (Versteeg and Malalasekera, 2007)

No. of extra transport equations	*Name*
Zero	Mixing length model
One	Spalart–Allmaras model
Two	k–ε model
	k–ω model
	Algebraic stress model
Seven	Reynolds stress model

The model that will be used in this study is the two transport equations, k-ϵ model. This model is the most commonly used in CFD modelling, and is used to compute the mean flow for turbulent flow characteristics. As it is shown in table 2.3 it is a two equation model. The two variables in the model is the turbulent kinetic energy k and the second is the turbulent dissipation rate ϵ.

$$\frac{\partial(\rho k)}{\partial t} + \mathrm{div}(\rho k \mathbf{U}) = \mathrm{div}\left[\frac{\mu_t}{\sigma_k}\,\mathrm{grad}\; k\right] + 2\mu_t S_{ij} \,.\, S_{ij} - \rho\varepsilon \tag{2.7}$$

$$\frac{\partial(\rho \varepsilon)}{\partial t} + \mathrm{div}(\rho \varepsilon \mathbf{U}) = \mathrm{div}\left[\frac{\mu_t}{\sigma_\varepsilon}\,\mathrm{grad}\; \varepsilon\right] + C_{1\varepsilon}\frac{\varepsilon}{k} 2\mu_t S_{ij} \,.\, S_{ij} - C_{2\varepsilon}\rho\frac{\varepsilon^2}{k} \tag{2.8}$$

Cκ, Cμ, Cϵ, C1ϵ and C2ϵ are five adjustable constants that the equations uses to solve the turbulent flow (Versteeg and Malalasekera, 2007).

3 Methodology

In this chapter the process will be explained, from the converting of the original .dwg file to the finished simulation in the CFD tool. Figure 3.1 shows the geometry from Autocad, this will later be reduced, more detail on this follows. The figure also shows the chosen flow direction for the simulation.

Figure 3.1: The flow direction

The wind rose of Oslo - Blindern is shown in figure 3.2, from this figure the dominant wind direction is determined to from the south west and to the north east. On this basis

the wind direction for the simulation is chosen.

Figure 3.2: The wind rose of Oslo, gathered from Meteorologisk Institutt

3.1 Building the 3D model

In order to relate the urban morphology with pressure coefficients, wind loads and air infiltration it is necessary to perform a CFD simulation in Star CCM+. This requires a 3D model of the area which is considered to be representative of the buildings and neighbourhoods in Oslo. The base of the geometry in the simulation is a SOSI file provided from "Kartverket" in Norway, this was converted to .dwg file before it could be adjusted in Autodesk Autocad. SOSI is the national standard for geographical information in Norway, it is widely used as a file format for Norwegian map data.

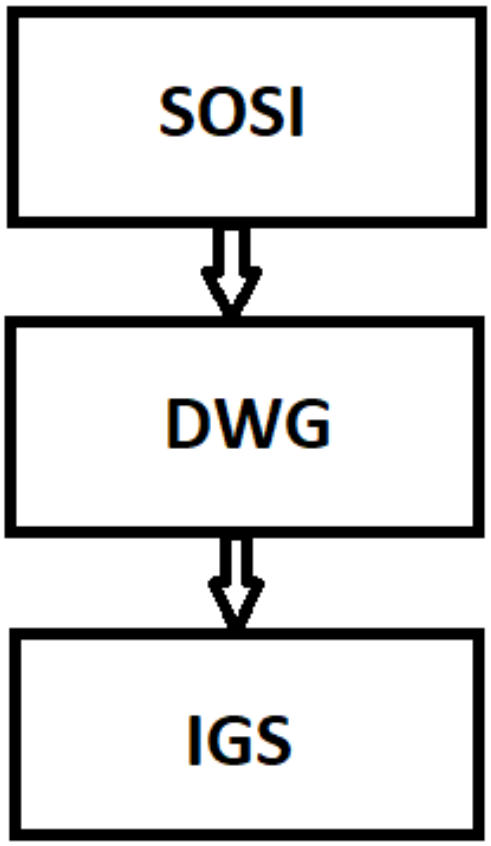

Figure 3.3: The workflow from SOSI to .igs

Figure 3.3 shows the workflow, from the original base file format, SOSI to .igs, more on that later in chapter 3.2.1.

At this point the area of the simulation was chosen, the focus was to be able to fit most of the building types of Oslo in the same geometry as that would then represent the actual

wind conditions in Oslo. The width of the geometry is around 600 meters, there are some variations to allow whole buildings and blocks to be fitted in the model. The length of the geometry spans from Barcode down by the sea in downtown Oslo all the way to Årvoll, on the way different types of buildings are represented in the different neighbourhoods. The wind in Oslo comes from the south-west, therefore the geometry has an angle of 30°NE as shown in figure 3.2. From the sea there are newly raised high-rises with the older apartment block followed by varying areas with parks, low-rise buildings and high-rise buildings. This achieves the idea of getting a good representation of all building types in Oslo and a good idea of the wind conditions within. The original .dwg file was brimming with information, much of it not useful in this case and causing trouble with extruding the geometry. In order to fix the problems with extruding in an easy manner the .dwg was cleaned. This means that all data outside of the chosen area was removed and the amount of information within the area was reduced. The file from Kartverket includes information connected to everything a modern city consist of; traffic, electricity, water and wastewater etc. A lot of this was removed beforehand but some of the information remained in the .dwg file. This caused the file to be large and slow to work with, all of the lines and information other than that of the outline of the buildings were removed to make the extrusion process smoother.

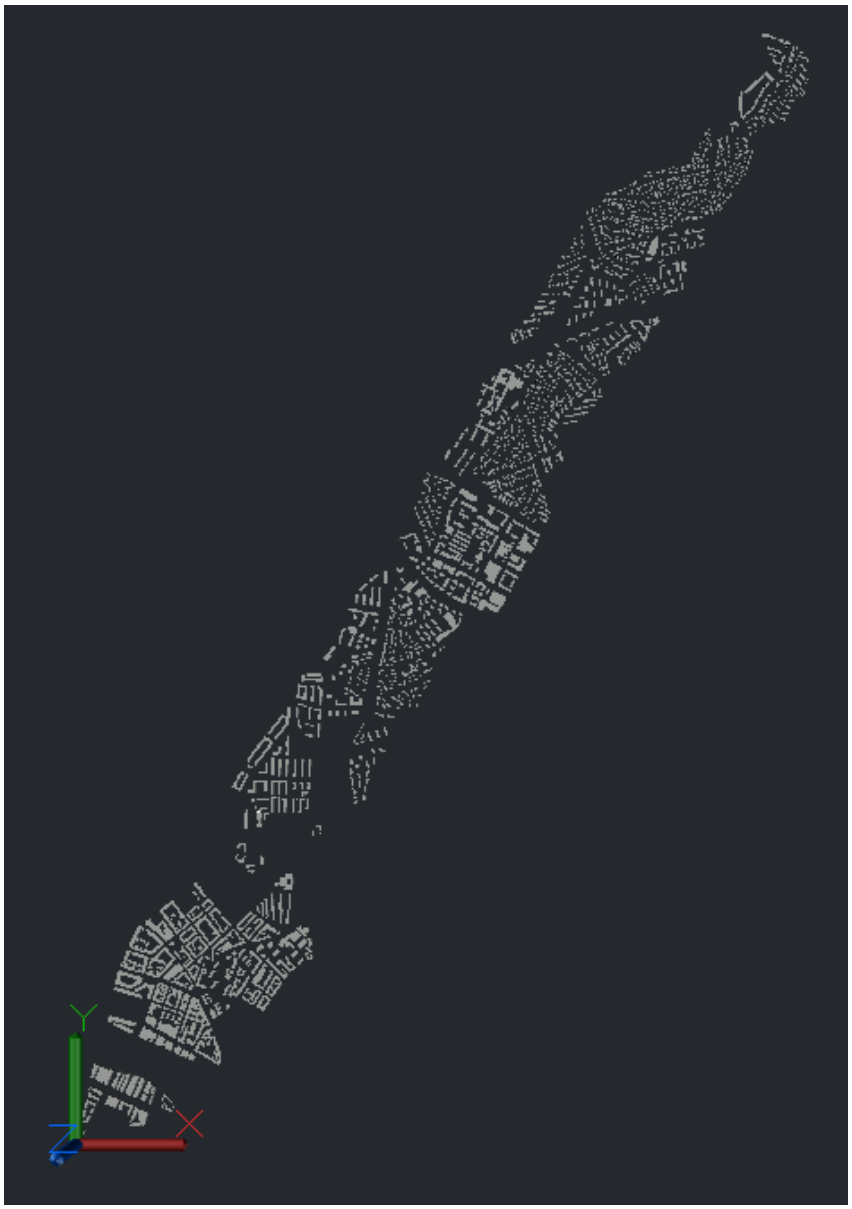

Figure 3.4: The geometry area as built in Autocad

After taking the aforementioned measures the extrusion was done and the result is shown in figure 3.4. Some simplifications was necessary in order to complete the geometry, this is as follows:

- Floor height set to 3 meters
- Same height for similar buildings in some areas
- Roof geometry set to flat
- Small buildings as sheds etc. is not in the model

In order to finish the geometry it was necessary to deal with some simplifications as shown above. The floor height was set to 3 meter for all of the building types, this way a 3-floor house is 9 meter and a 4-floor house is 12 meter, with this simplification the extrusion of the model can be done within an agreeable time limit. Another simplification related to the building height is that similar buildings in the same neighbourhoods were set to the same height, with some exceptions when there are buildings that differ greatly from the norm in the neighbourhood. In Oslo there are a lot of different roof geometries, this is chosen as flat for all roof types. This would have an effect on the wind, but looking at the time it would have taken to model all the roofs this was simplified. Around the building blocks and houses there are smaller construction such as sheds, bus shelters and newsstands, these smaller buildings were not extruded and removed from the geometry. This was done to reduce the size of the extrusion task and also because they would have had a negligible effect on the wind.

In the end the geometry was reduced to ensure that the import to the CFD tool worked, see details in chapter 3.2.1. The final geometry with the regions labeled is shown in figure 3.5.

Figure 3.5: The geometry with labeled regions

3.2 Star CCM+

Star CCM+ is a tool developed by Simcenter and it is used to complete multiphysics solution for products and conditions. One of the physics solution it can be used for and will be used for in this case is CFD - simulation. The methodology in terms of the settings in the CFD tool will be explained later in the chapter.

3.2.1 Import of geometry

The next step was to export the geometry from Autodesk Autocad to a format that Star CCM+ would be able to import. This involved several attempts in order for the import of the geometry to be successful. Star CCM+ can read .iges from Autocad and parasolid files from Inventor. Initially none of these files worked as intended, as the geometry in Star CCM+ showed as points only and not solid surfaces. This was because of the coordinate system in the original .dwg file. Originally, the 2D sketch of Oslo is large as consist of all of Oslo and surrounding areas. This caused the UCS, the coordinate system to be way of base when a lot of the geometry had been removed. Relocating the origin of the .dwg file to a more central area for the current geometry fixed the importing issues. However, when this was taken care of it was discovered a restriction of a maximum geometry cube size of 1000 meter. In order to get this to work with the current geometry there are three options;

1. Use a smaller part of the geometry
2. Scale down the geometry
3. Divide the geometry in four regions and run four simulations

When using a smaller geometry it will be more challenging to implement all building types and the relation between urban morphology and the aspect ratio of street and buildings. To scale down the geometry also presents new challenges, one of them is that the wind will also need to be scaled down to be appropriate with the scaled geometry. The last option is to divide the geometry in four regions, by doing this the maximum restrictions is not going to be a problem but some extra work will occur with the additional simulations.

The solution to the alternatives was to divide the geometry into different regions. This

would most accurately represent the different kinds of building types in Oslo and therefore more accurately simulate the wind conditions within the model. An important aspect of this alternative is to be mindful of the transition between the regions. The start conditions in the following regions must conform with the output from the former region. This is an essential part in order to get the simulation accurate. In order to get the transition correct, the use of file table has been used to transfer the velocity from one region to the next. This is done by creating a plane section in the already simulated region, this section must be located after the buildings and then extract the velocity values and export the table. The next step is to import this file table in the next region and apply it to the inlet surface. The plane section and the inlet surface must match, so that the distance from the buildings is accurate. As mentioned earlier Star CCM+ has a maximum geometry restriction on 1000 meter cube size. That means that the imported regions from AutoCad must be limited to 600-800 meter, this is because there must be left some room for the wake in the domain geometry. In region 1 and 2 there is also necessary to have some room between the inlet and the first buildings, but this is not the case with the rest of the regions because of the density of the buildings in this part of the geometry.

From the original geometry shown in 3.4 there are modelled 5 regions consisting of high-rise buildings by the seaside and low-rise buildings deeper into the city. The regions is shown in the following regions, where the first one is region 1, then region 2 and so forth.

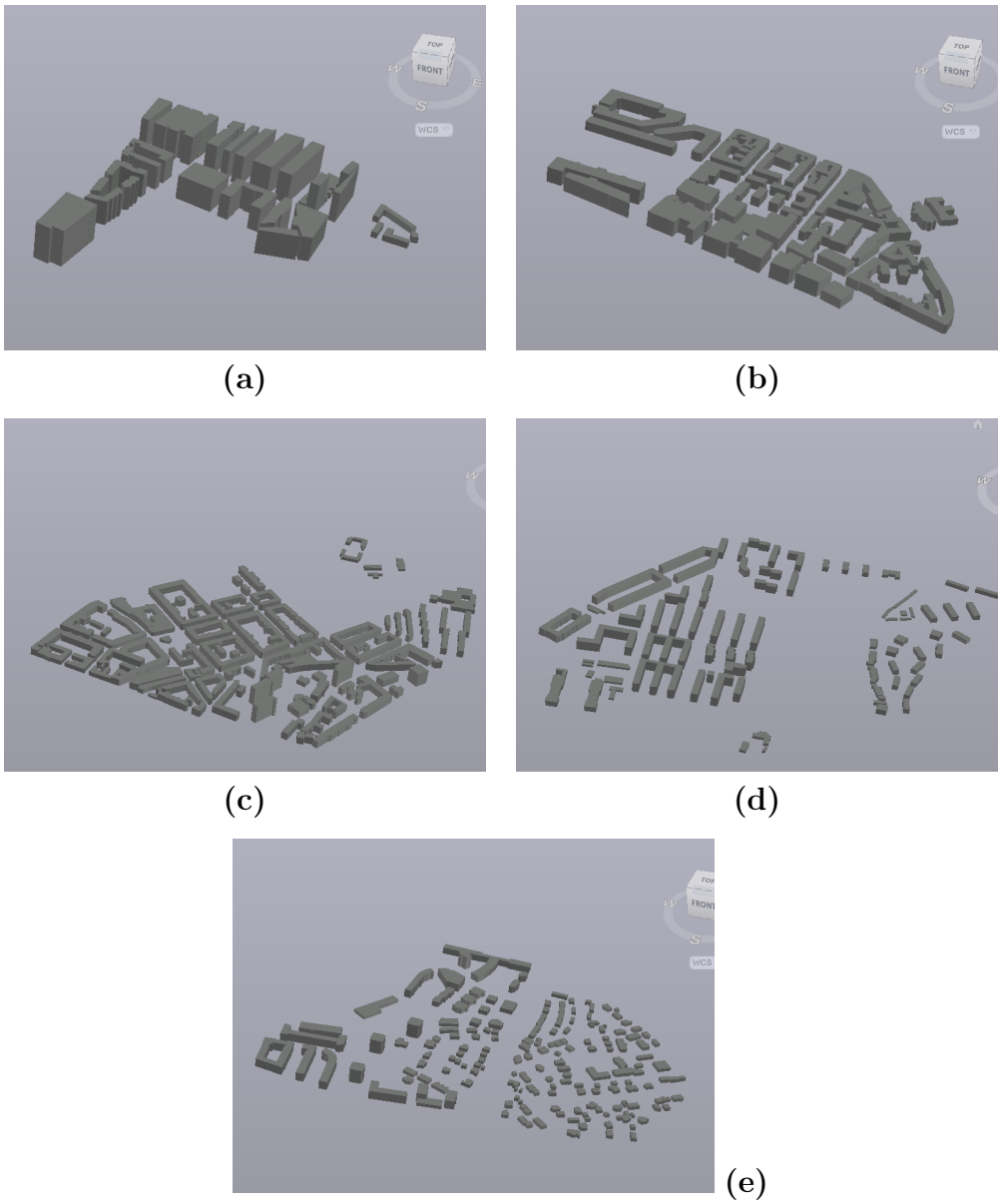

Figure 3.6: **(a)** Region 1 **(b)** Region 2 **(c)** Region 3 **(d)** Region 4 **(e)** Region 5

With the geometry imported into Star CCM+ the following points will be done in order to run the simulation in each region;

1. Model domain
2. Subtract buildings and domain
3. Set up the mesh
4. Set up the physics
5. Run simulation

After importing the geometry the next step is to generate the mesh. In order to to that the geometry needs a domain around it. A box is modeled around the buildings, making sure it is enough space between the walls of the domain and the edge of the buildings. If this space is too small, it is a risk that the building will grow into the domain wall when the meshing model is run.

3.2.2 Meshing models

Looking at the total geometry it is clear that some parts of the model will need more attention when it comes the size of the meshing cells, this mesh refinement makes it necessary to divide the region in different boundary regions.

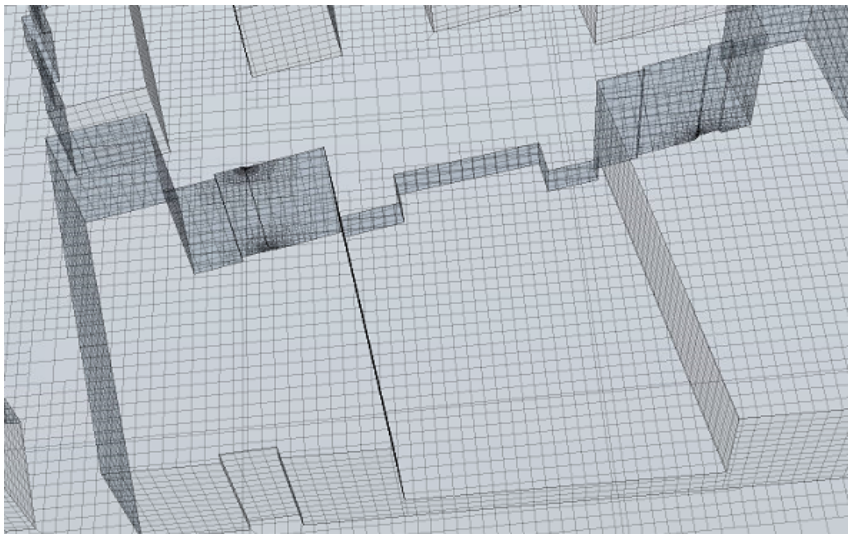

Figure 3.7: Mesh with problems in details

In order to achieve the best possible mesh several options where tried and tested. The first option was whether to go with tetrahedral or polyhedral mesh, then you have several reference values to test to get the optimal mesh. A lot of testing was done with different base size on the geometry, and testing with the wrapper scale factor. In figure 3.7 a repeating problem is shown. The geometry looks mostly fine, but there are issues with details in some corners of the building. This is probably due to some properties that have transferred over from the .sosi file, the file from Kartverket mentioned in 3.1. This issue was mostly fixed when the right value for the wrapper scale factor was discovered and applied.

There will be different needs for meshing size when considering the domain geometry and

the actual buildings within the domain, as illustrated in figure 3.8. Because of this the region is divided in several boundaries in Star CCM+, one for the buildings and one for the domain. The domain is again divided in different boundaries to have control of the air flow, more of this later.

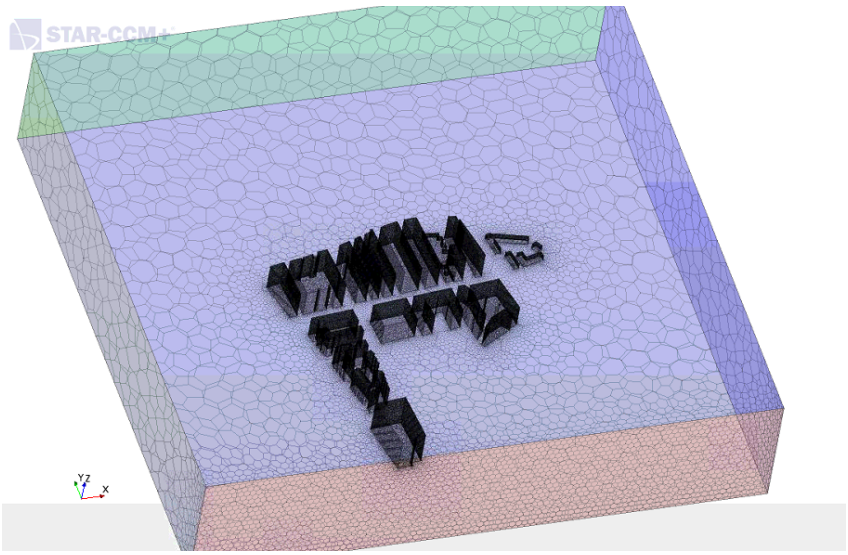

Figure 3.8: From mesh in region 1

It is essential to get a good mesh in order to get accurate results when running the simulation but it is also important when considering the overall size of the file. If the file size is too big, i.e. very small meshing size on the whole geometry the simulation will take a long time to run. By managing the meshing size one can achieve a more sensible file size and simulation process. A geometry with the same meshing size on the whole model is not preferable because different areas of the model requires different attention when considering mesh. Small details as pockets in the wall will need smaller meshing size than a 20 m^2 wall. Because of this it is important to have the meshing size to change according to where the details in the geometry is. From figure 3.8, it is shown the difference in mesh size. The buildings have a rather fine mesh size and the domain surrounding the buildings is more course. The boundary growth rate is an option in Star CCM+ which is set to "fast", this to make the cells change from small to large quickly and vice versa.

When the correct settings for the mesh options was set, the same recipe was applied for all the regions. The recipe was as follows.

1. Models; Polyhedral mesher

2. Surface remesher
3. Surface wrapper
4. Reference values; Base size - 50 meter
5. Surface size [percent], relative minimum - 0.1, relative maximum - 100
6. Wrapper scale factor [percent] - 15

In mesh continua set up these values are chosen and, the rest of the options available were left at default values. In addition to these settings, it is necessary to set some personalized settings for the boundaries. The roof, outlet and walls surfaces was left as is. But the rest of the surfaces needed custom surface size settings. These were as follows.

1. Buildings [percent] - rel. min. 0.1, rel. max. 2.0
2. Floor [percent] - rel. min. 0.1, rel. max. 100
3. Inlet [percent] - rel. min. 0.1, rel. max. 20

Below, in figure 3.9, the meshes for the five regions are shown. In terms of the domain it is the same size, but the geometry inside varies in terms of quantity of buildings and height and size of the buildings.

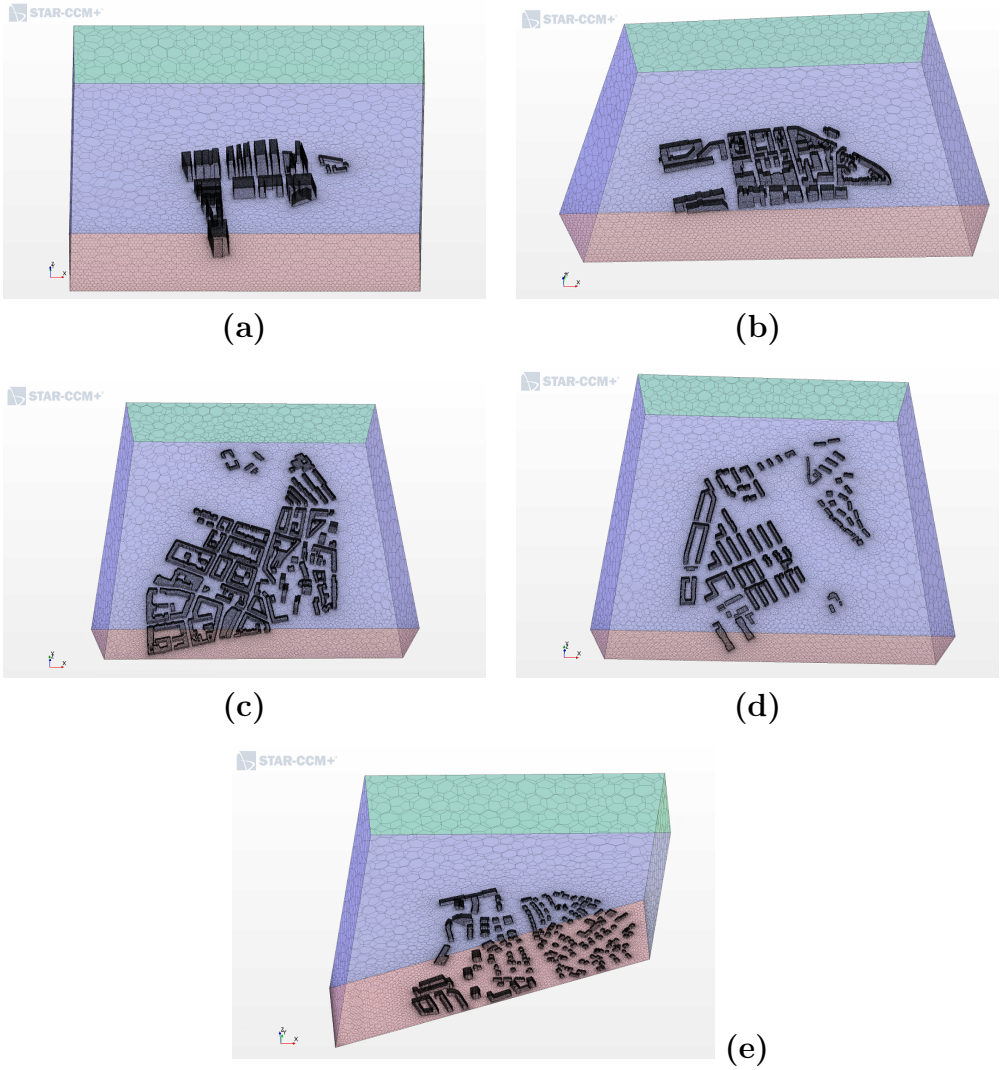

Figure 3.9: **(a)** Region 1 **(b)** Region 2 **(c)** Region 3 **(d)** Region 4 **(e)** Region 5

The five regions varies when considering how much time the meshing process took. As shown in table 3.1 the largest region in terms of building mass demanded the most, and has the highest number of meshing cells. The other four regions were similar in time and cells.

Table 3.1: Overview of the time spent meshing each region and the total cells in the mesh

Region	Total cells	Wall time [seconds]
1	2 187 985	6 275.48
2	2 348 640	6 506.06
3	4 943 247	15 370.33
4	2 432 083	6 723.83
5	1 936 158	5 753.57

3.2.3 Boundary Conditions

The boundary conditions in a domain governs the flow, on the five regions that is simulated a power law has been applied in the inlet and the conditions applied to the other surfaces on the domain decides how the flow will work. When choosing the type of boundary condition to apply to a surface there are several options, in order to accurately depict the real flow situation it is important to set these boundaries as correctly as possible. The different boundaries are shown with labels in figure 3.10 below.

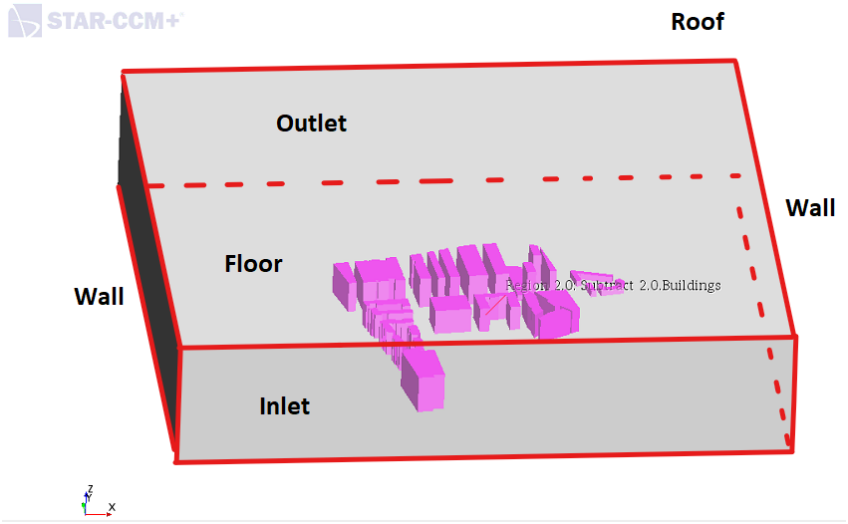

Figure 3.10: The boundaries shown in region 1

As mentioned the inlet has a power law flow condition in the first region. In the following regions the inlet boundary is determined by an XYZ table from the previous region, this is to achieve the same flow throughout the five regions. The outlet boundary condition is set as an "outlet" in Star CCM+, this boundary represents an outflow condition without

any back-flow (Simcenter, 2020). This can be used when dealing with a computational domain that only has outward directed flow. The walls and roof of the domains is set as symmetry planes. Finally the floor and the building surfaces in the domain is set as walls, with the no-slip condition. "No-slip" means that the fluid moves with same velocity as the wall and sticks to it (Simcenter, 2020). This means that when dealing with stationary walls the velocity is zero along the building surfaces.

3.2.4 Physics in the model

The following physics models are chosen for the simulation. From figure 3.11 it is shown the enabled physics models in Star CCM+.

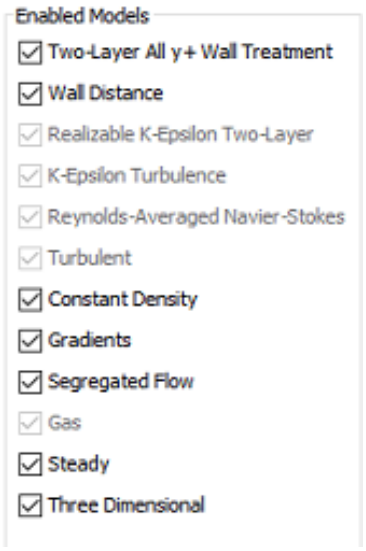

Figure 3.11: Enabled physics models

Most notable is the decision to go with the K-Epsilon turbulence model. The fluid in the model is air at constant density and with segregated flow. The simulation will be a steady - state simulation.

4 Results

There has been simulated five regions with many buildings in total. There are many options regarding what kind of results to extract and analyse. In this chapter results from the five regions will be presented which later will be compared and discussed. A comparative study will be performed considering pressure coefficients on the building facades and the velocity within the city.

4.1 Region 1

Region 1 is located right next to Oslofjorden, that means that the wind has no obstacles before it hits the first building in the region. The region has high-rise buildings and is a part of a newly built region in Oslo called Barcode.

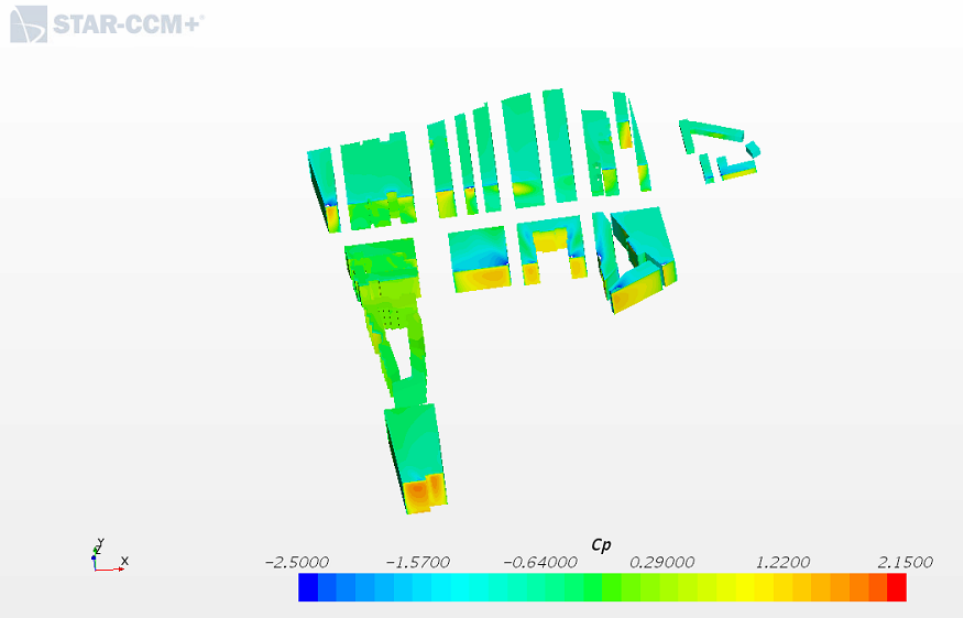

Figure 4.1: Pressure coefficients in Region 1

From figure 4.1 the situation regarding the pressure coefficients in region 1 is shown. The flow direction is along the Y-axis and it is clear from looking at the figure that the highest Cp values occur on the building facades where the wind first hits directly from the sea.

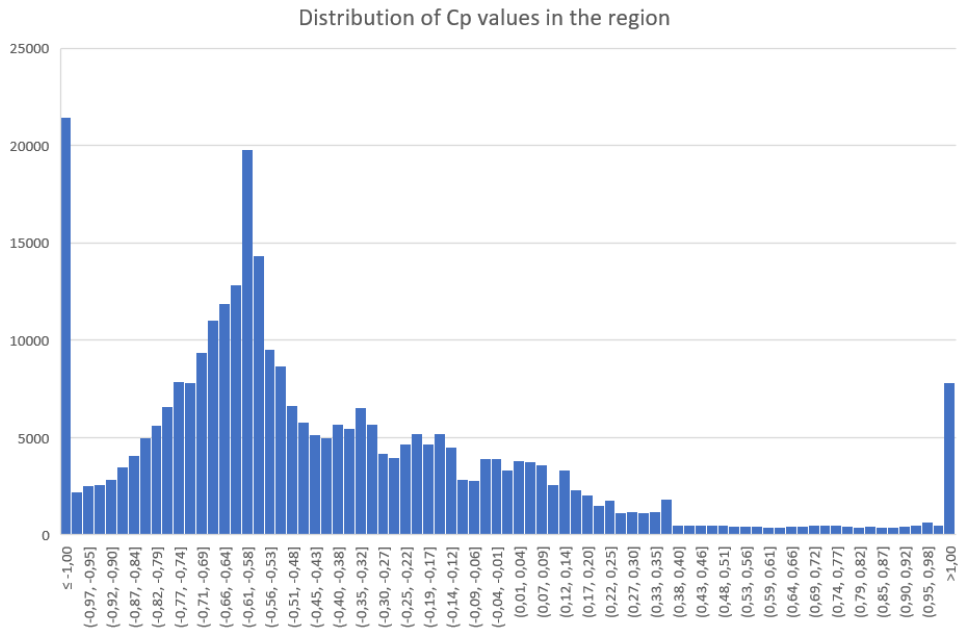

Figure 4.2: Distribution of the Pressure coefficients in Region 1

Figure 4.2 shows the pressure coefficient distribution in all the points on the building surface in region 1. It shows the distribution of the Cp values in the region. The average Cp value is -0.420. This is due to a number of points where the Cp is as low as -4, the highest value is 1.7. The range of the histogram is -1.0 to 1.0, most of the pressure coefficients is -0.9 and 0.1.

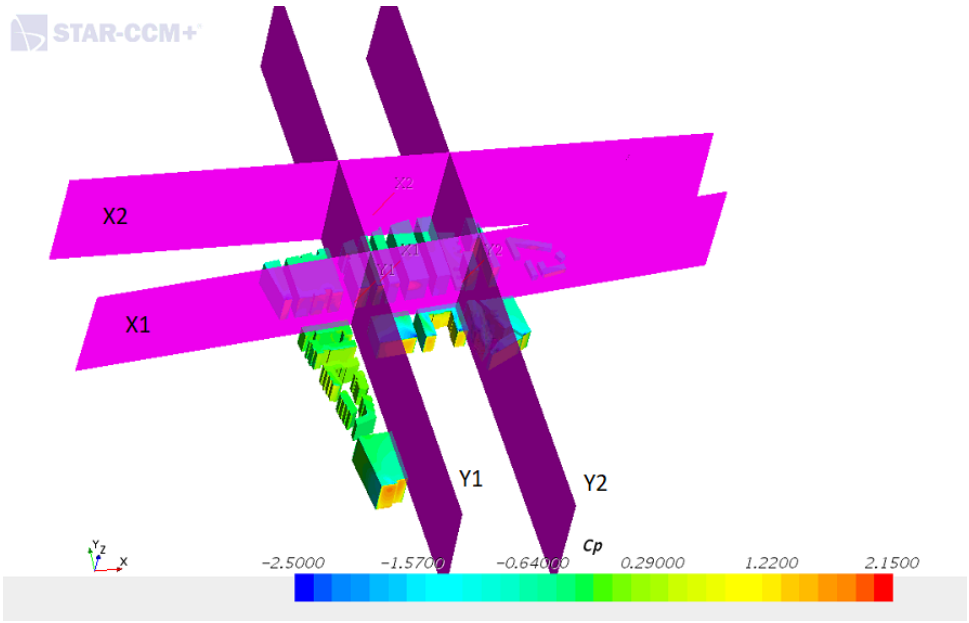

Figure 4.3: The location of the sections in Region 1

Figure 4.3 shows the location of the plane sections in region 1. The sections have been

named X1, X2, Y1 and Y2 for function analysis. The X-sections are the planes normal to the flow direction and the Y-sections are the planes along the flow direction. X1 is located in the main street separating the buildings in this region, X2 is a plane directly after the buildings in the region. Y1 is the one on the left following a street and Y2 is the one on the right following a parallel street.

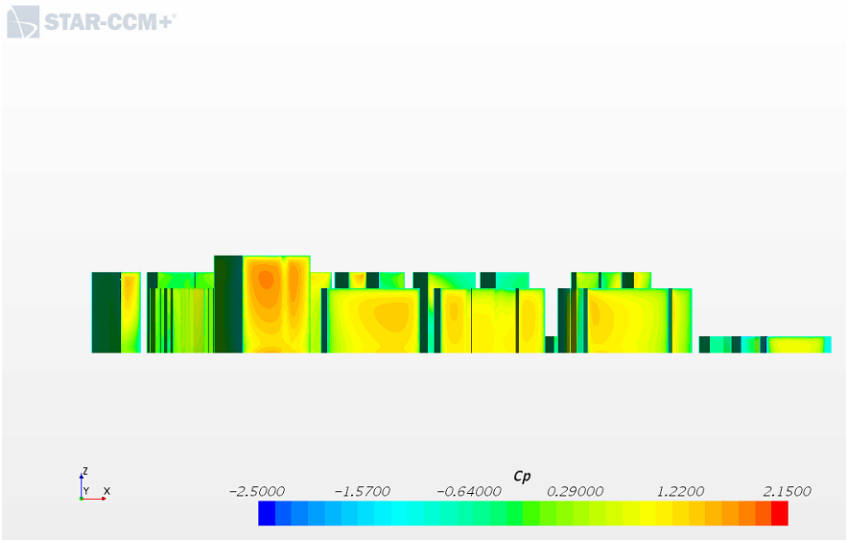

(a)

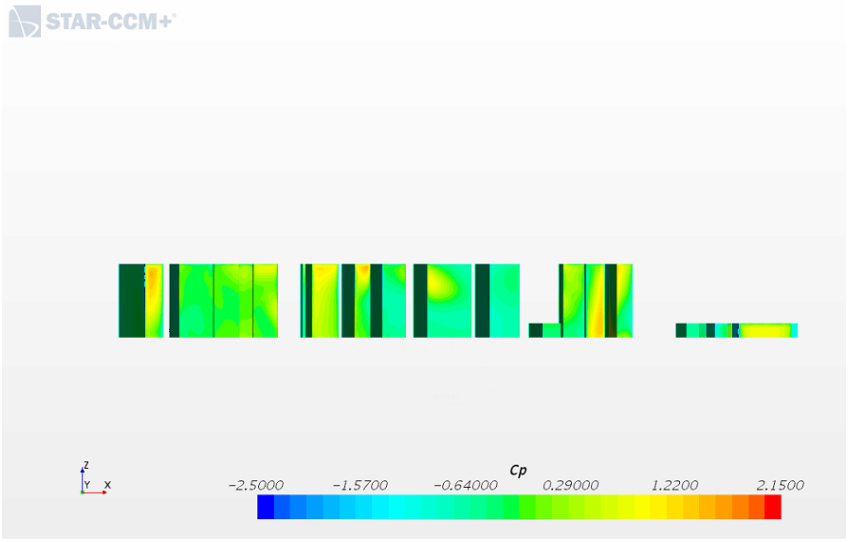

(b)

Figure 4.4: **(a)** The pressure coefficients in section X1 in Region 1 **(b)** The pressure coefficients in section X2 in Region 1

Figure 4.4 shows the pressure coefficients in the sections normal to the flow direction. Image a) depicts how it looks from the front that is completely exposed to the wind from the sea. It is in this section the highest pressure coefficients occur. The section behind,

image b) shows that the pressure coefficients is relatively lower as these surfaces are not directly exposed to the wind.

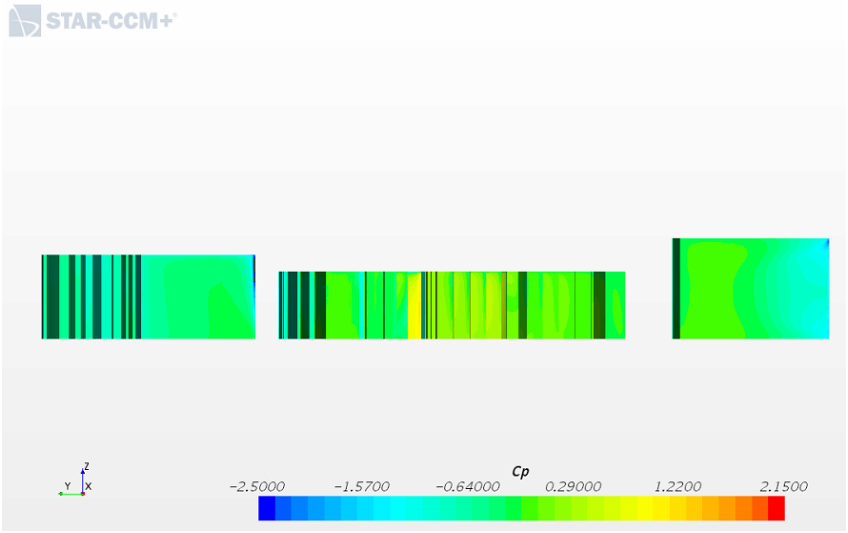

(a)

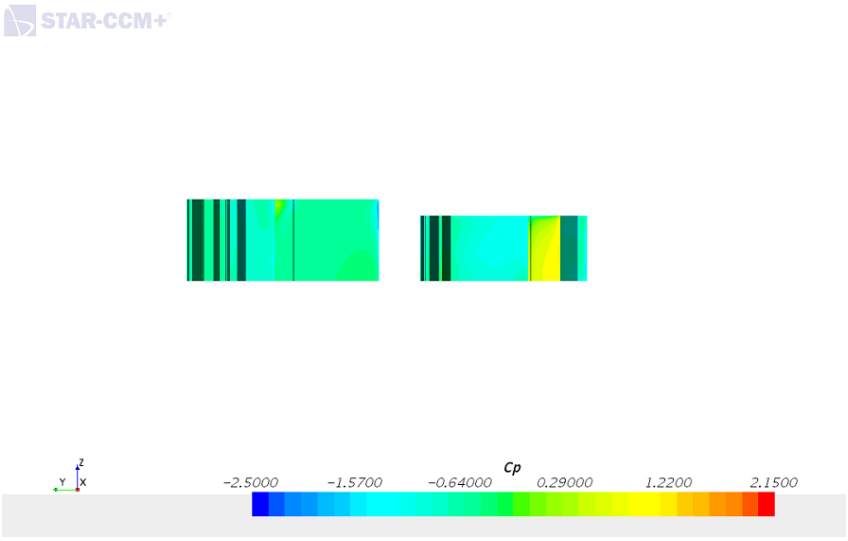

(b)

Figure 4.5: **(a)** The pressure coefficients in section Y1 in Region 1 **(b)** The pressure coefficients in section Y2 in Region 1

Figure 4.5 shows the two section along the flow direction. In both image a) and b) the flow direction is along the Y-axis, to the left in the images. From both sections negative pressure coefficients occur on the sides of the building surface exposed to the wind. The negative values is lesser deeper in the geometry.

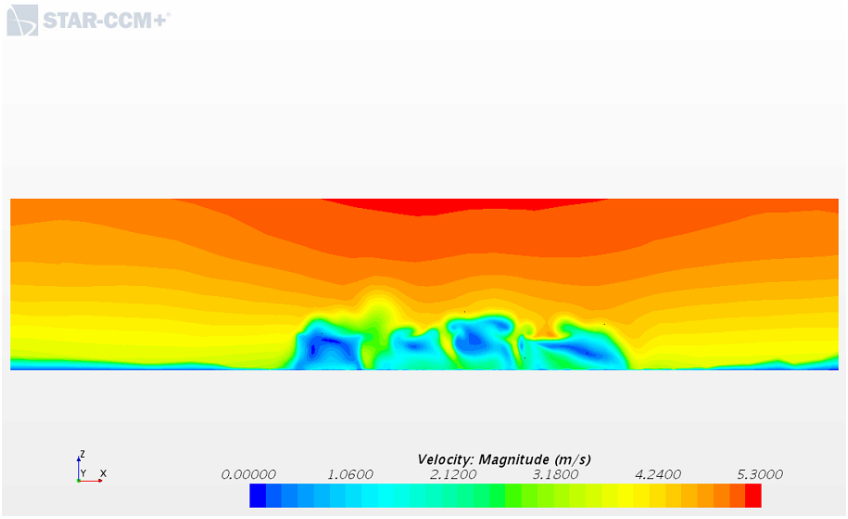

(a)

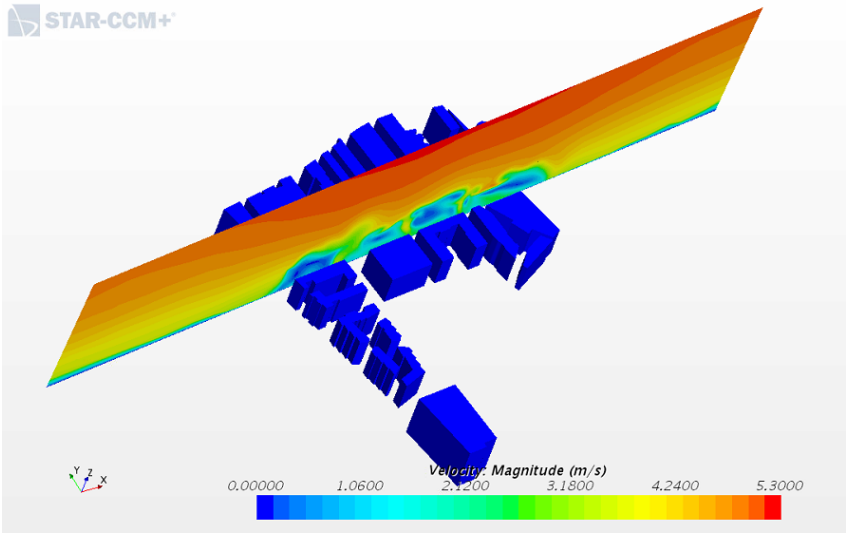

(b)

Figure 4.6: **(a)** The velocity shown in section X1 in Region 1 **(b)** The location of section X1 shown in the first image

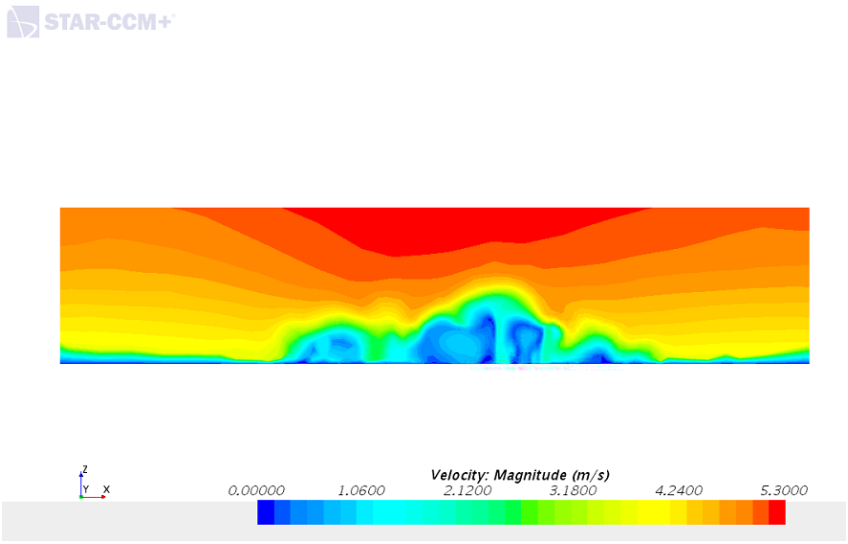

(a)

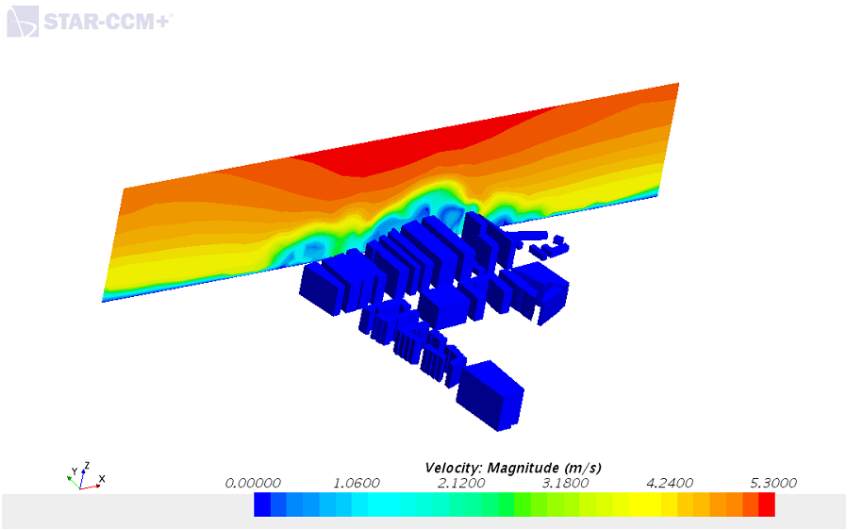

(b)

Figure 4.7: **(a)** The velocity shown in section X2 in Region 1 **(b)** The location of section X2 shown in the first image

Figure 4.6 and 4.7 shows the velocities in the sections normal to the flow direction. The power law clearly comes into effect because the velocity is generally higher at the top of the section plane. It is the most variety in values between the buildings in the planes in X1. The same can be observed in plane X2 where the velocity is less behind the buildings.

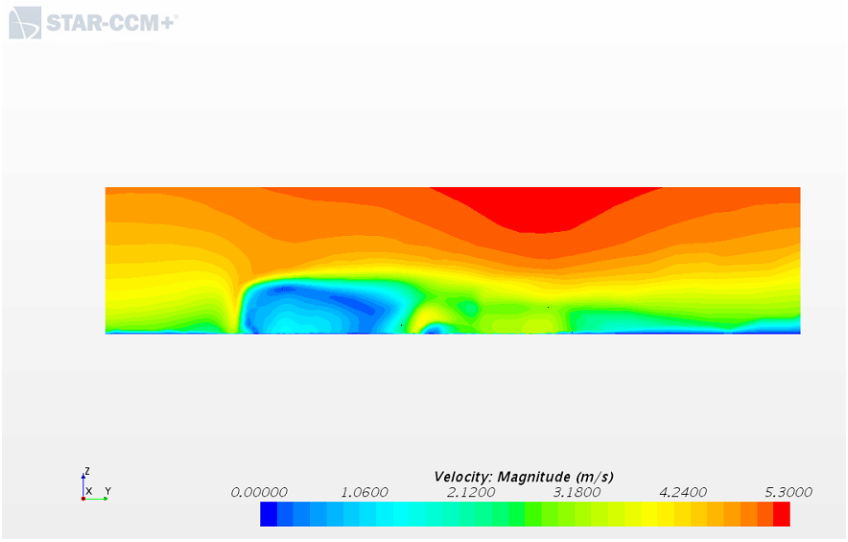

(a)

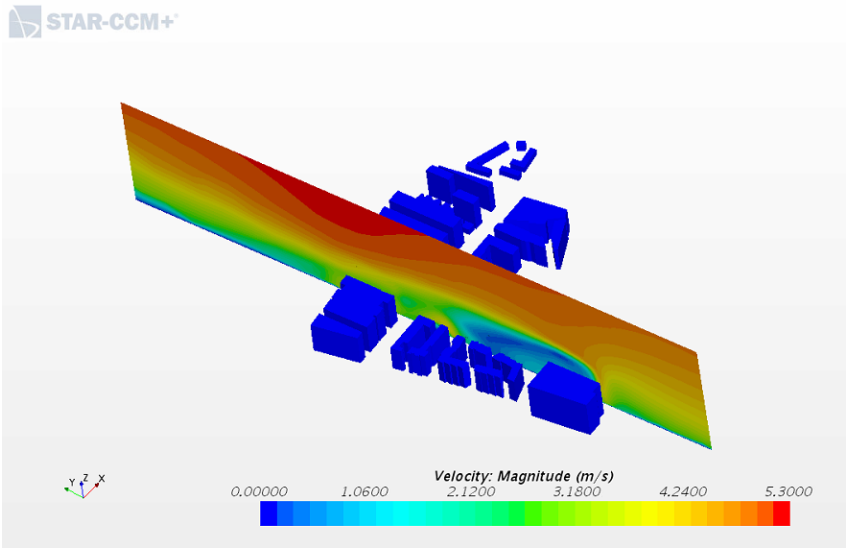

(b)

Figure 4.8: **(a)** The velocity shown in section Y1 in Region 1 **(b)** The location of section Y1 shown in the first image

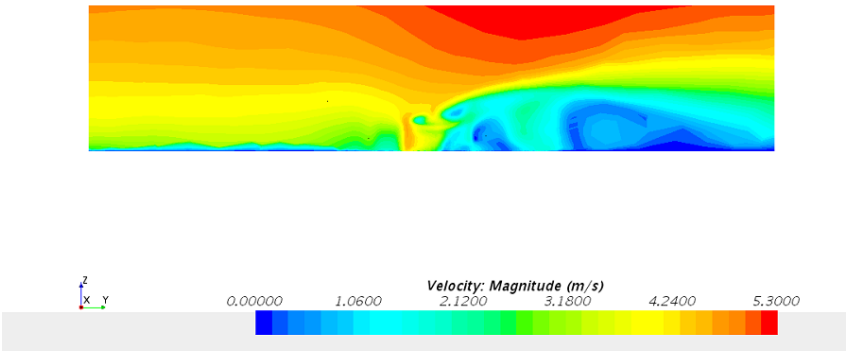

(a)

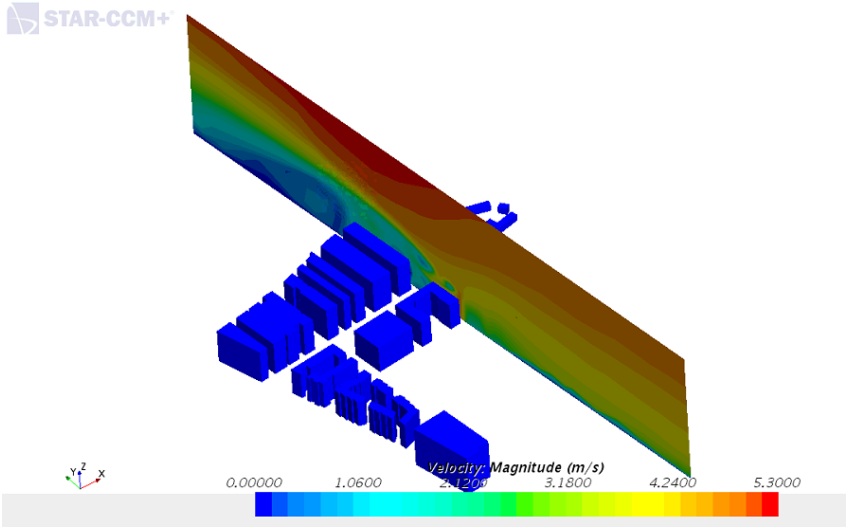

(b)

Figure 4.9: **(a)** The velocity shown in section Y2 in Region 1 **(b)** The location of section Y2 shown in the first image

Figure 4.8 and 4.9 shows the velocities in the sections along the flow direction. The two sections is placed in the canyons between the buildings to see how the velocity will behave in these conditions.

4.2 Region 2

The railway that goes to Oslo central station is located between region 1 and 2, this area is approximately 150 meters long. This gap provides the wind with the opportunity to stabilize to some extent before it reaches the buildings in region 2. The region consist of old apartment buildings that ranges from 10 to 15 meters.

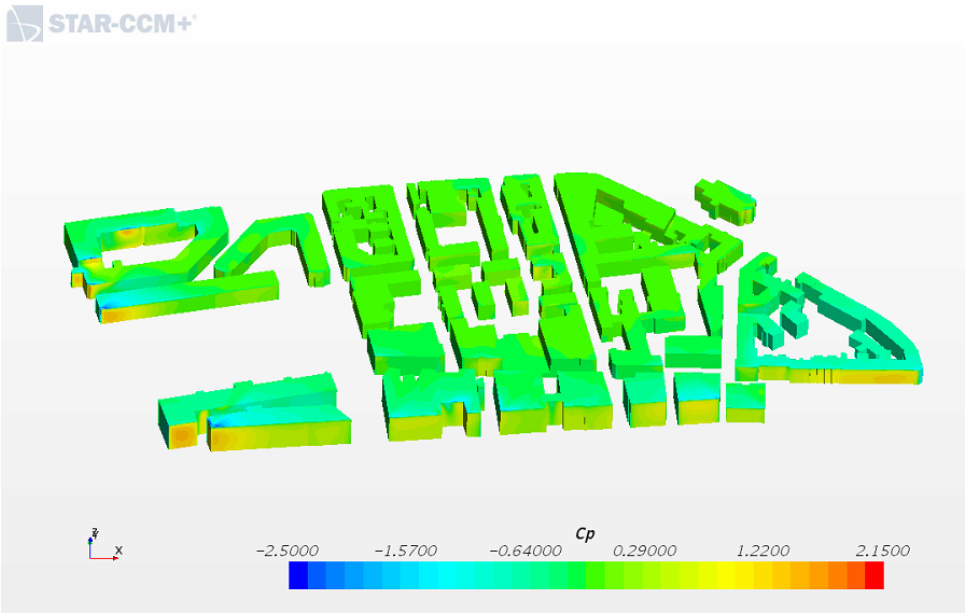

Figure 4.10: Pressure coefficients in Region 2

Figure 4.10 shows the pressure coefficients in region 2. The building facades normal to the wind direction is the surfaces most exposed to the wind, as is shown by the pressure coefficients on these surfaces.

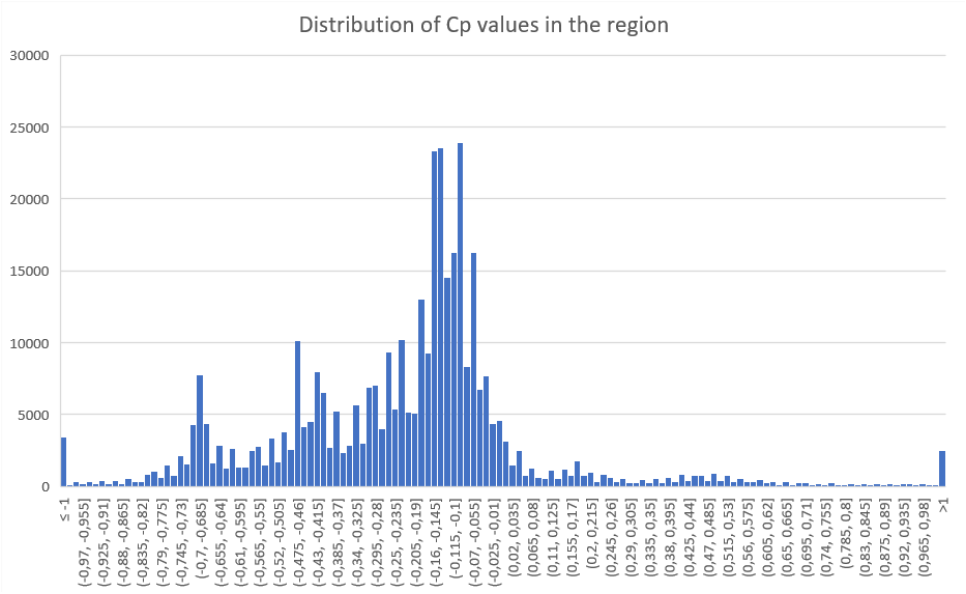

Figure 4.11: Distribution of the Pressure coefficients in Region 2

The flow direction is along the Y-axis, the highest Cp value is 1.5 and the lowest is -4. The average Cp is -0.219, the negative value is because of the few very low values some places in the buildings. The distribution of the Cp values is shown in figure 4.11. The majority of the pressure coefficients lies between -0.7 to 0.

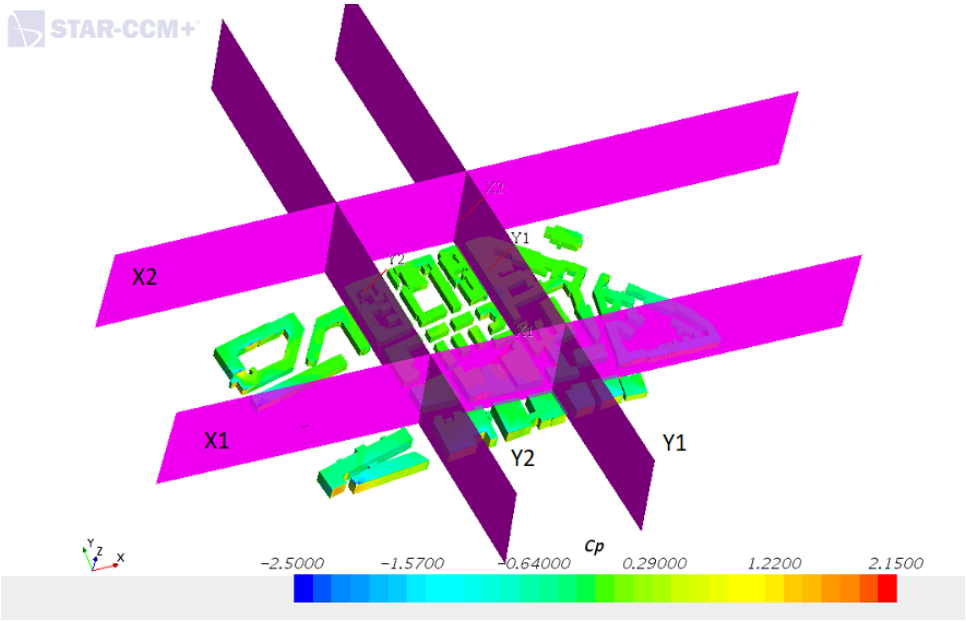

Figure 4.12: The location of the sections in Region 2

The locations of the sections in region 2 is shown in figure 4.12. The four sections is named X1, X2, Y1 and Y2 with the sections named X normal to the flow direction and

the sections named Y along the flow direction. X1 is placed on the street behind the first row of buildings and X2 is placed behind the last row of buildings. Y1 is placed in a street to the right in figure 4.12 and Y2 is placed in a street to the left.

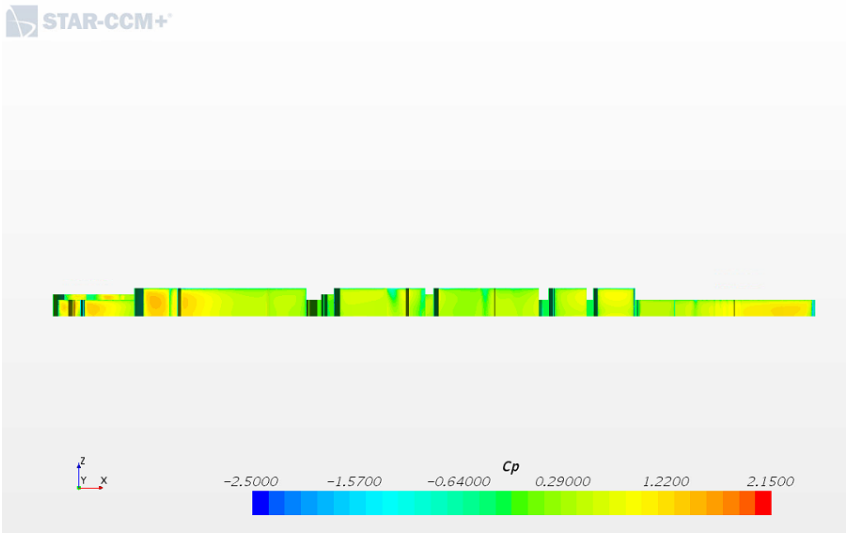

(a)

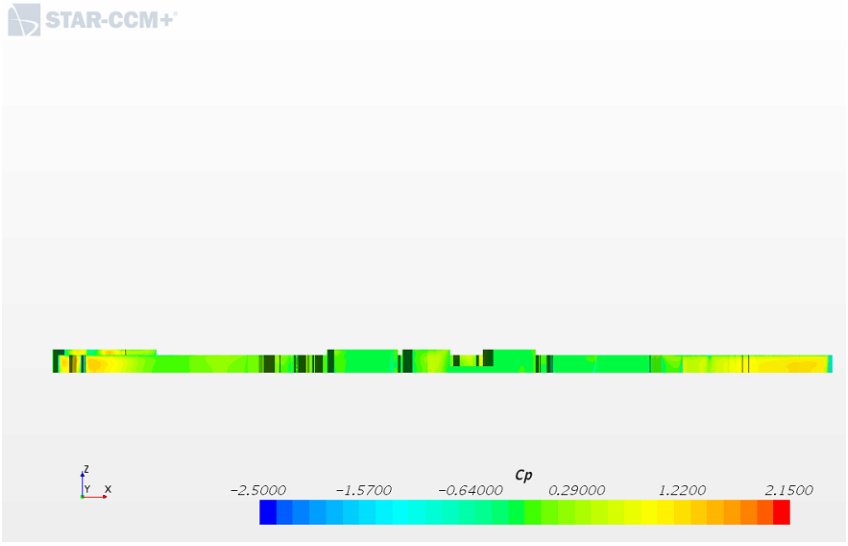

(b)

Figure 4.13: **(a)** The pressure coefficients in section X1 in Region 2 **(b)** The pressure coefficients in section X2 in Region 2

Figure 4.13 shows the two sections where the flow is normal to flow direction. Image a) shows the first row of buildings in the region. Between region 1 and 2 there is open space where the railway is located, this ensures that the buildings are exposed to the wind. From image b) the pressure coefficients in the middle buildings are much lower. The side buildings in image b) still do not have any cover and the pressure coefficients have not

changed from image a).

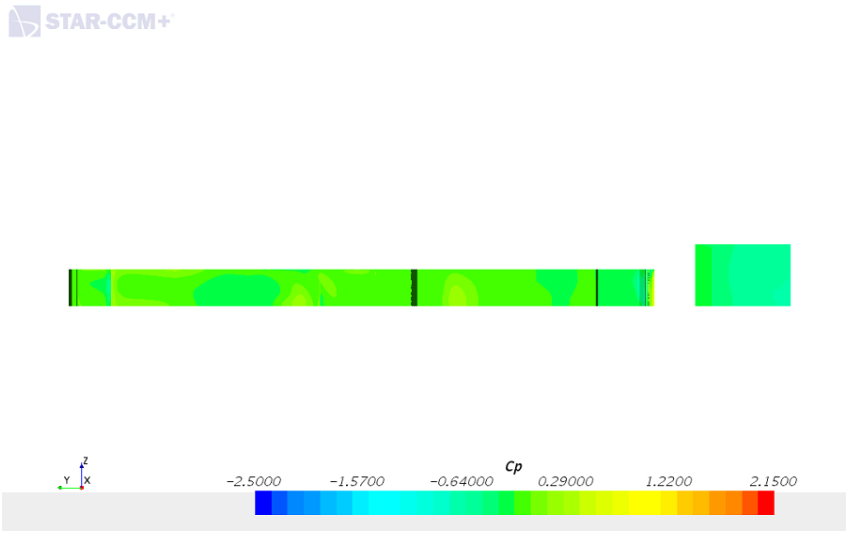

(a)

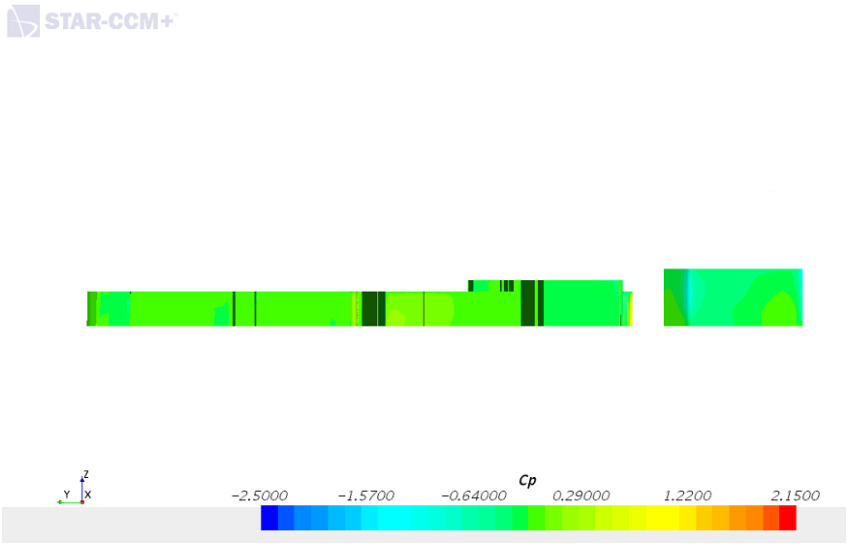

(b)

Figure 4.14: **(a)** The pressure coefficients in section Y1 in Region 2 **(b)** The pressure coefficients in section Y2 in Region 2

The two sections where the flow direction is along the section is shown in figure 4.14. These building surfaces are quite uniform in colour indicating that the pressure coefficients are not varying much.

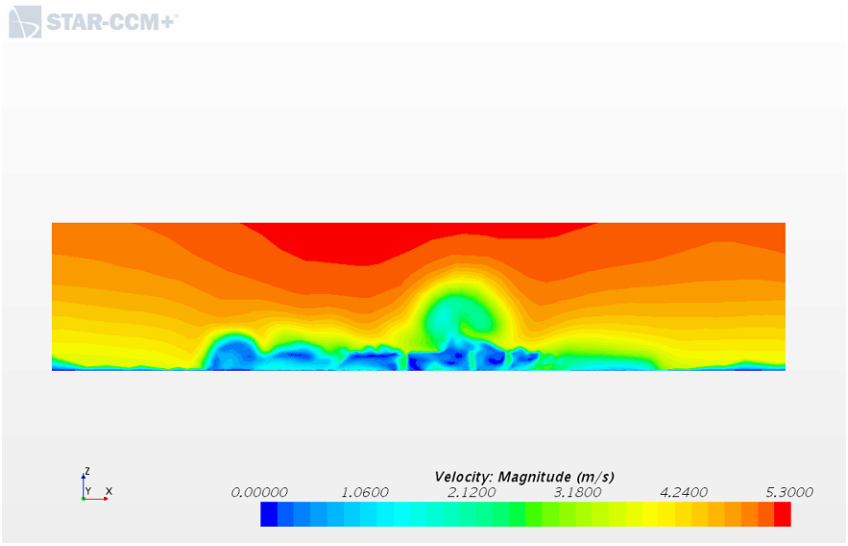

(a)

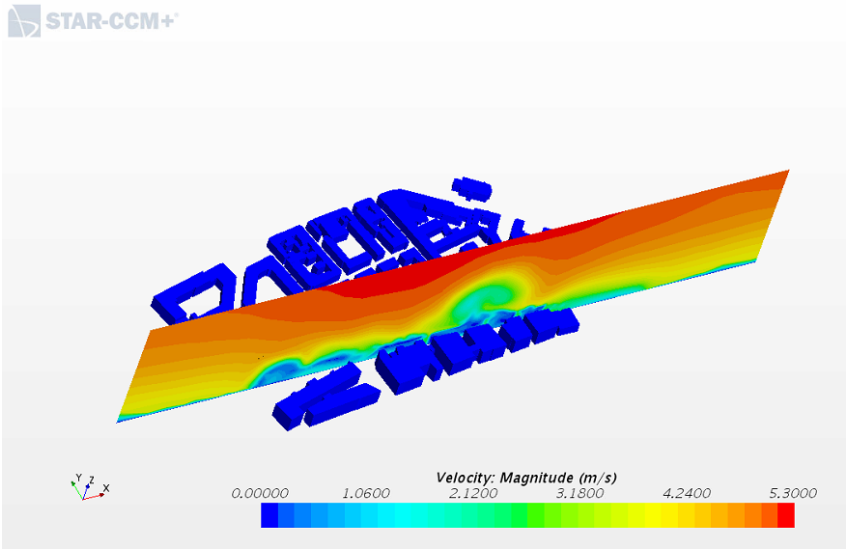

(b)

Figure 4.15: **(a)** The velocity shown in section X1 in Region 2 **(b)** The location of section X1 shown in the first image

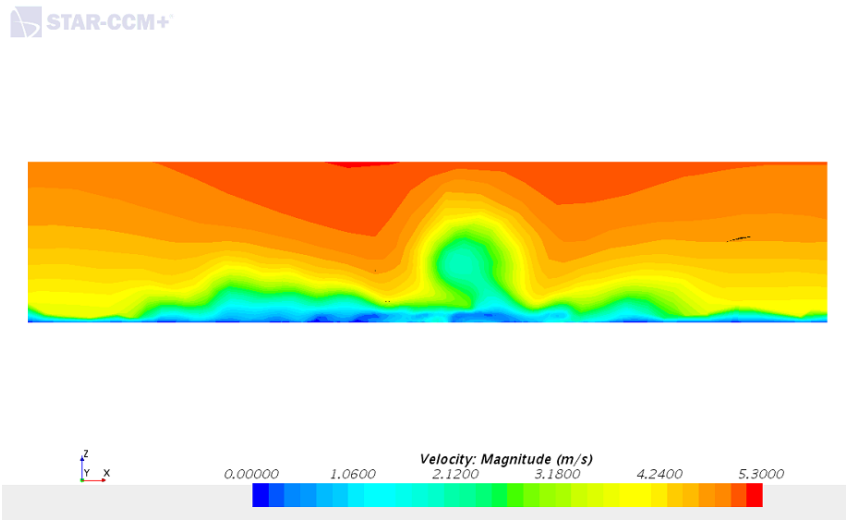

(a)

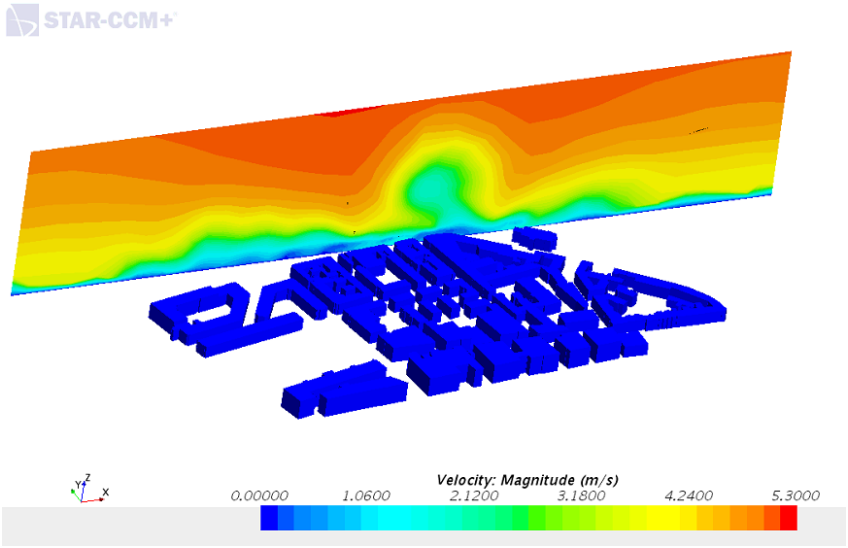

(b)

Figure 4.16: **(a)** The velocity shown in section X2 in Region 2 **(b)** The location of section X2 shown in the first image

Figure 4.15 and 4.16 show two sections normal to the flow direction in region 2. The first section, X2 is placed in the street behind the first row of buildings to show the velocity magnitude in this canyon. The second section, X2 is placed behind the last buildings in the regions to see how the velocity magnitude is behind the region.

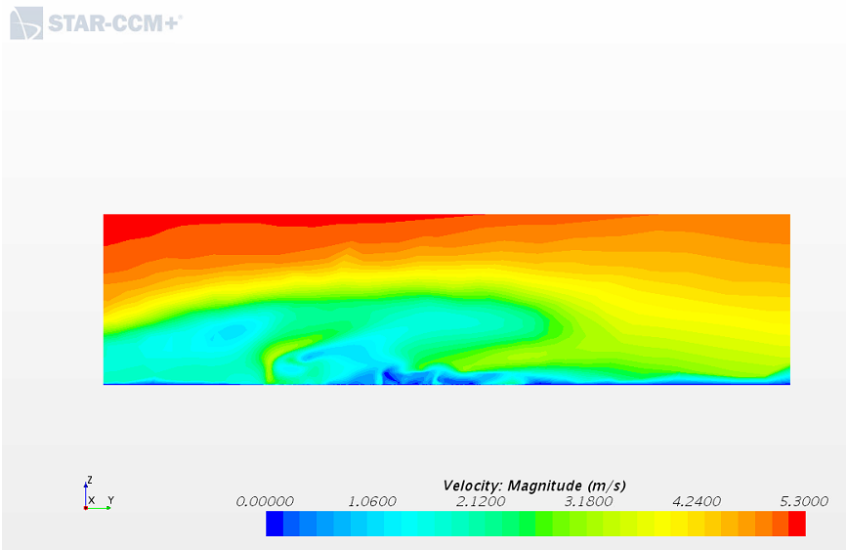

(a)

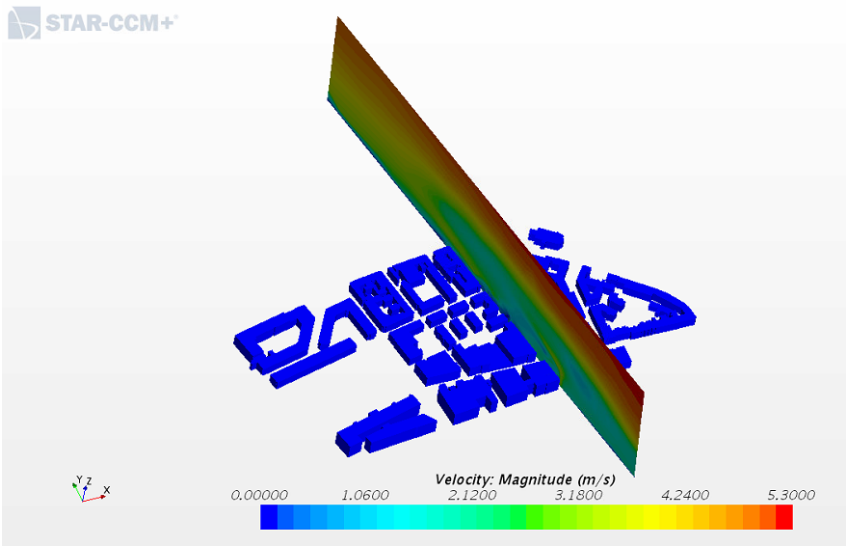

(b)

Figure 4.17: **(a)** The velocity shown in section Y1 in Region 2 **(b)** The location of section Y1 shown in the first image

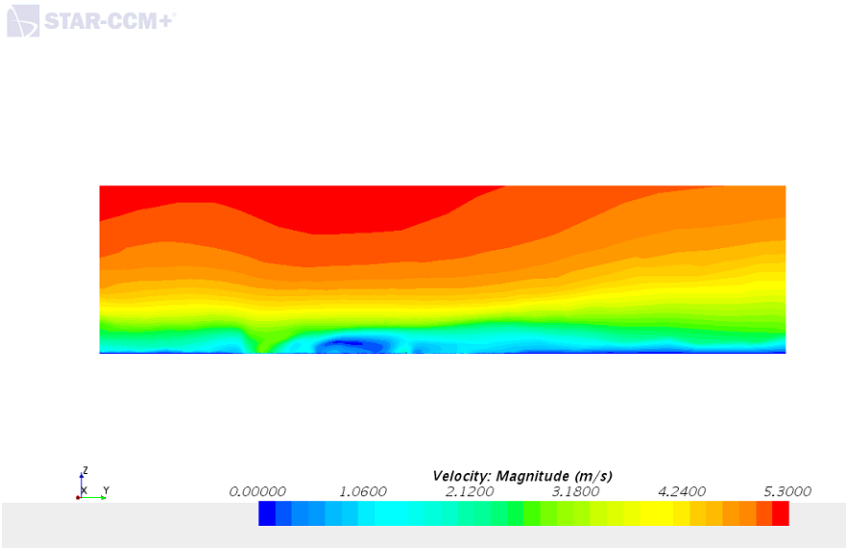

(a)

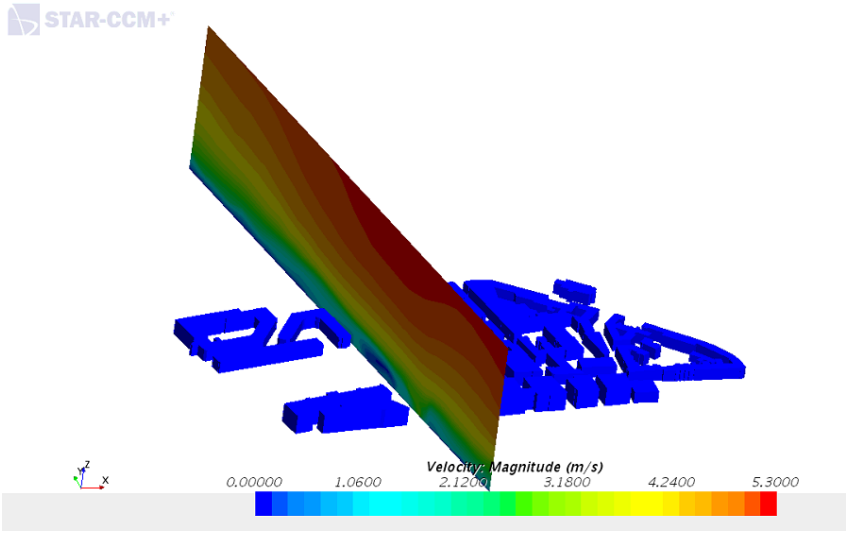

(b)

Figure 4.18: **(a)** The velocity shown in section Y2 in Region 2 **(b)** The location of section Y2 shown in the first image

Figure 4.17 and 4.18 shows the two sections in region two where the flow is along the flow direction. The two sections is placed in two separate streets, one street more open (Y2) than the other (Y1).

4.3 Region 3

Between region 2 and 3 there is only one street that divides the regions, the street is 20 meter wide. Region 3 is the largest region in terms of quantity of buildings. This can also be seen from table 3.1, where the number of cells is much larger than in the other regions.

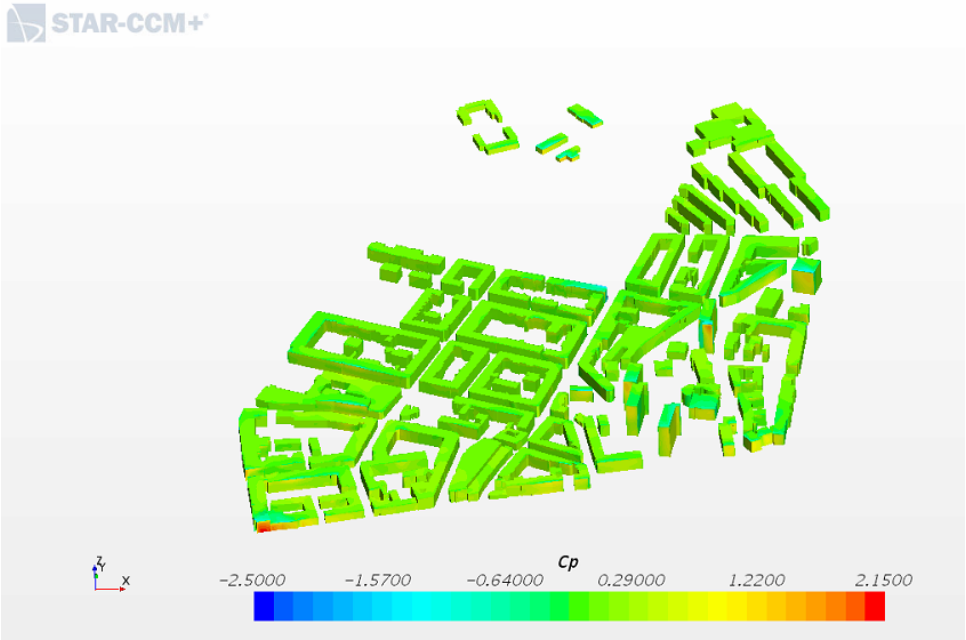

Figure 4.19: Pressure coefficients in Region 3

Figure 4.19 shows the pressure coefficients in region 3. From the figure it shows that the whole region and the Cp values are quite uniform overall. the exceptions are the tall buildings and the building facade on the left where the pressure coefficients are higher than the rest of the region.

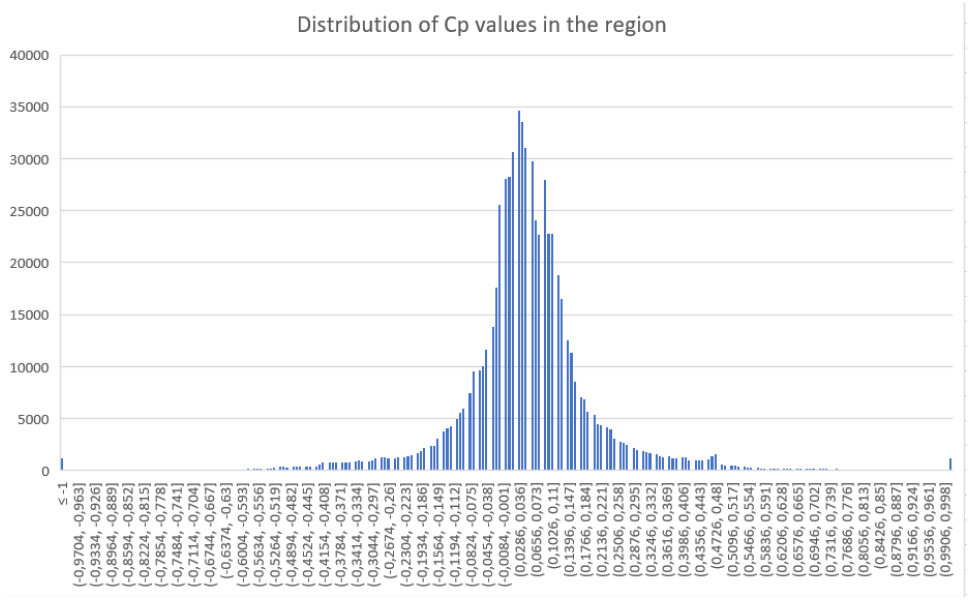

Figure 4.20: Distribution of the Pressure coefficients in Region 3

The highest Cp value of the region is 2 and the lowest is -4.4. The average Cp of the region is 0.051. In 4.20 the distribution of the Cp value is shown. The majority of the points lies between -0.20 and 0.30.

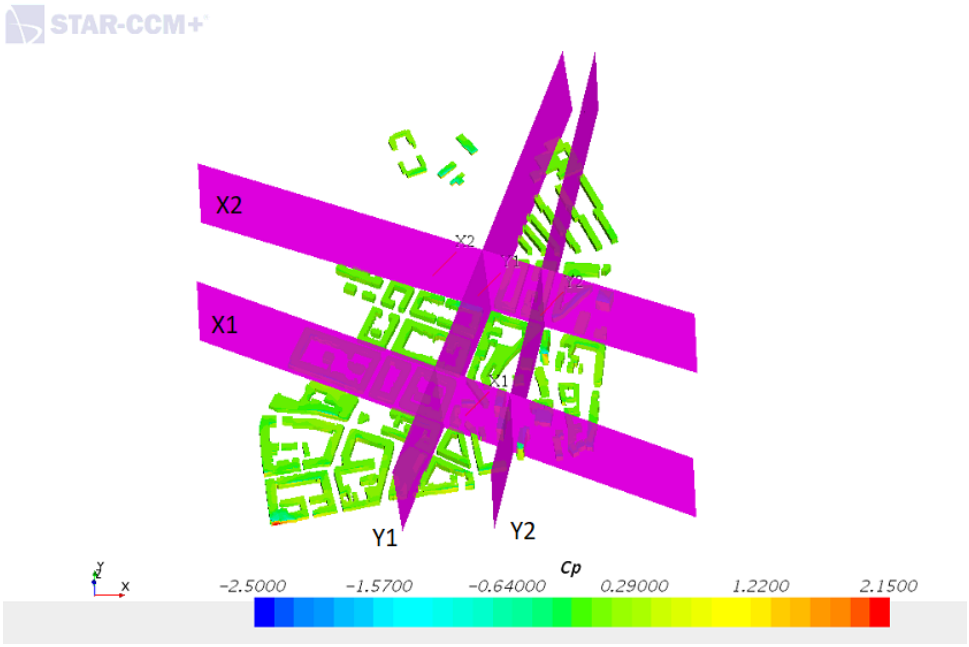

Figure 4.21: The location of the sections in Region 3

The four sections of this region is shown in figure 4.21, two section normal to the flow direction and two sections along the flow direction. All four sections is placed in the streets to see the difference in both pressure coefficients and velocity.

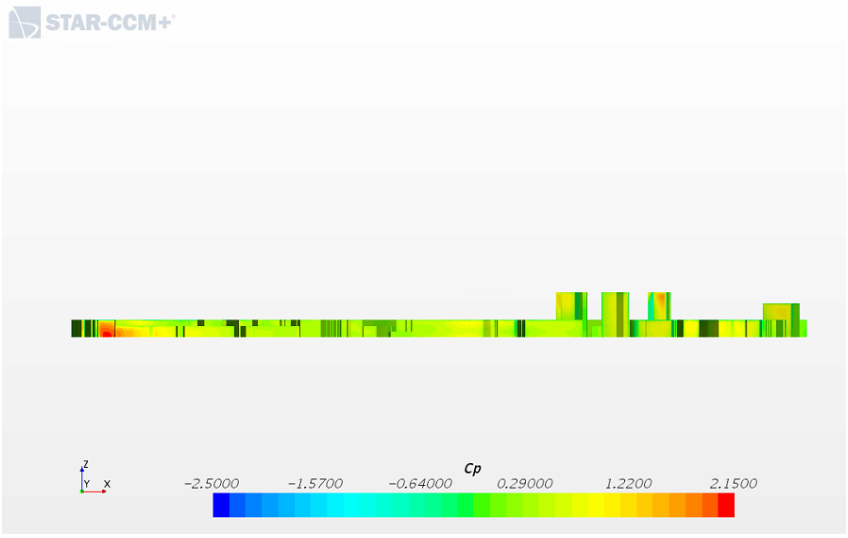

(a)

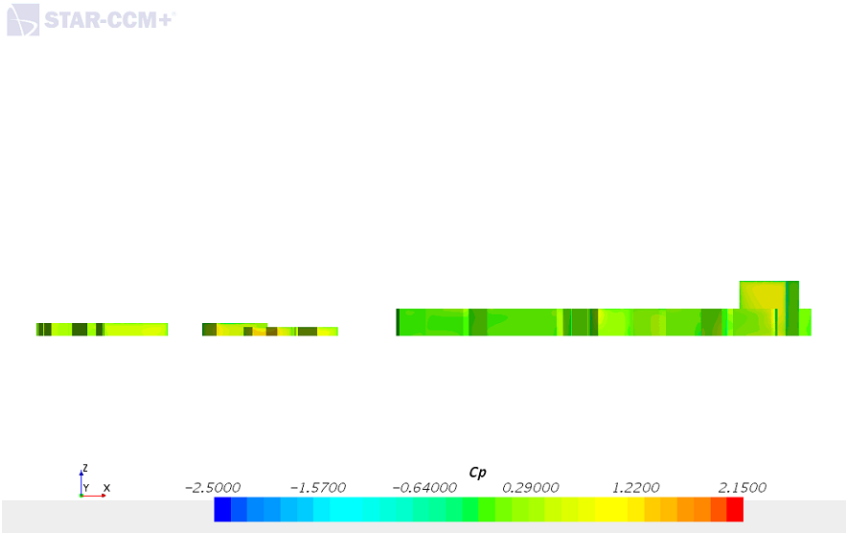

(b)

Figure 4.22: **(a)** The pressure coefficients from the front line of buildings in Region 3 **(b)** The pressure coefficients in section X1 in Region 3

The two sections shown in figure 4.22 shows the pressure coefficients in to planes normal to the flow direction. Image a) is the first row of buildings in the region. There is only a street separating region 2 and 3, and this shows on the pressure coefficients in image a). The front line is somewhat covered from the region before with the left side as an exception, this part is exposed from the previous region. Image b) is located at section X1 from figure 4.21. This row of building is even more covered in terms of wind and the pressure coefficients are low except for the left side and the one tall building on the right side.

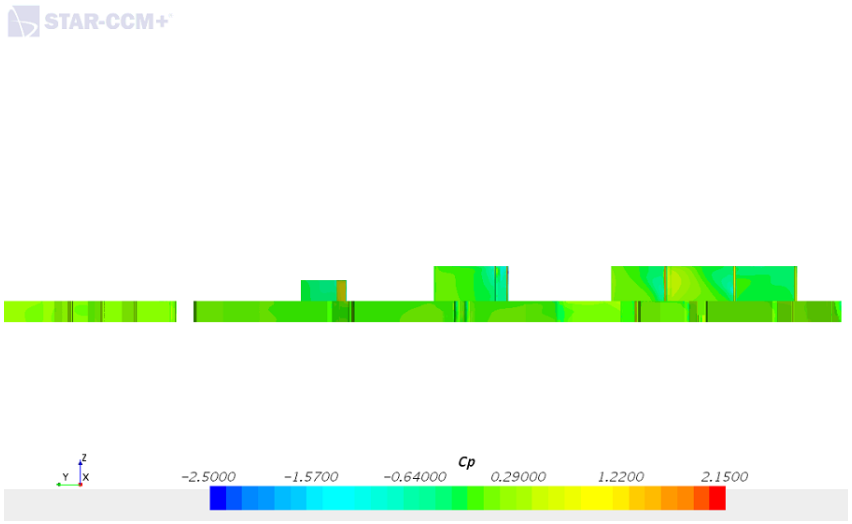

(a)

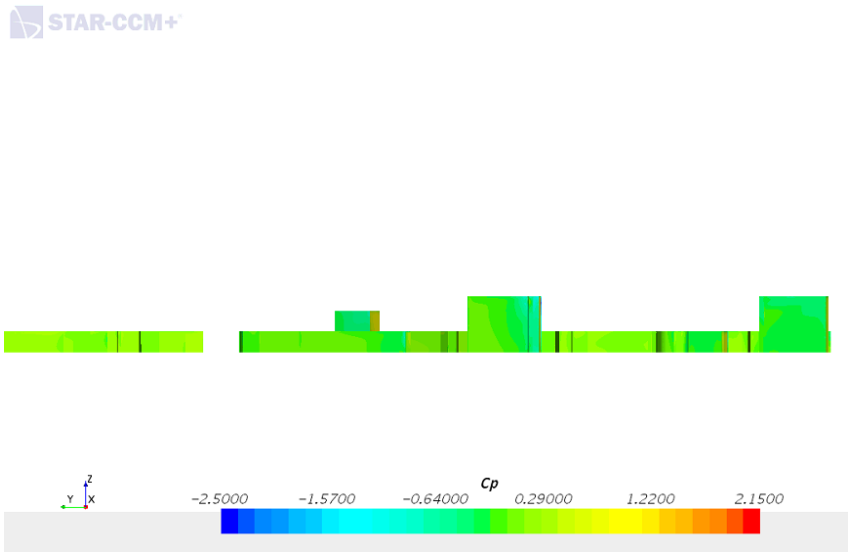

(b)

Figure 4.23: **(a)** The pressure coefficients in section Y1 in Region 3 **(b)** The pressure coefficients in section Y2 in Region 3

The to views in figure 4.23 shows two views who are along the flow direction. Image a) shows the section Y1 and image b) shows section Y2.

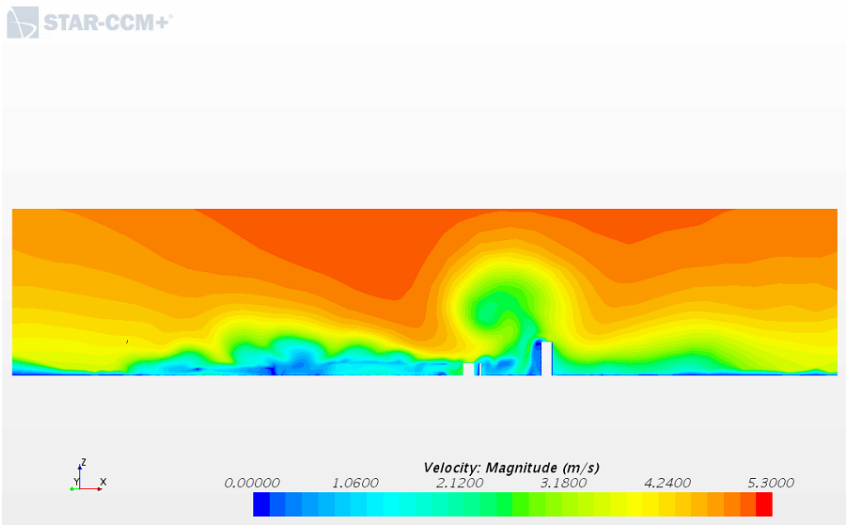

(a)

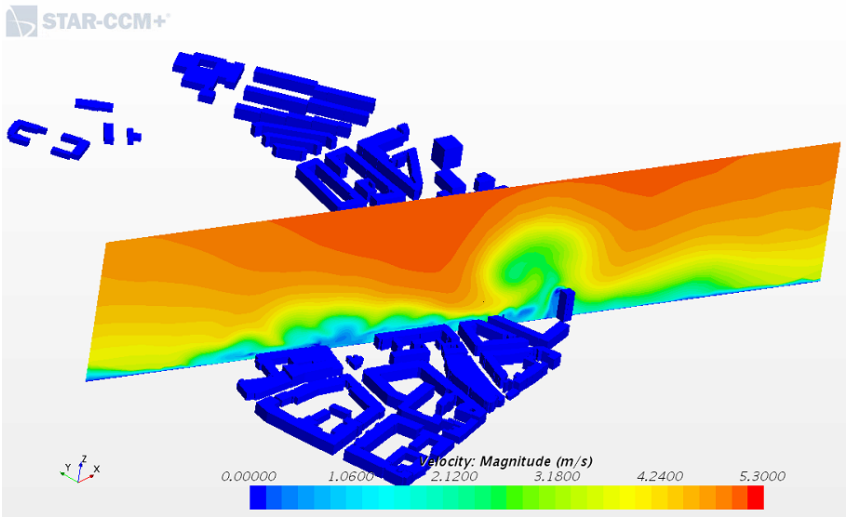

(b)

Figure 4.24: **(a)** The velocity shown in section X1 in Region 3 **(b)** The location of section X1 shown in the first image

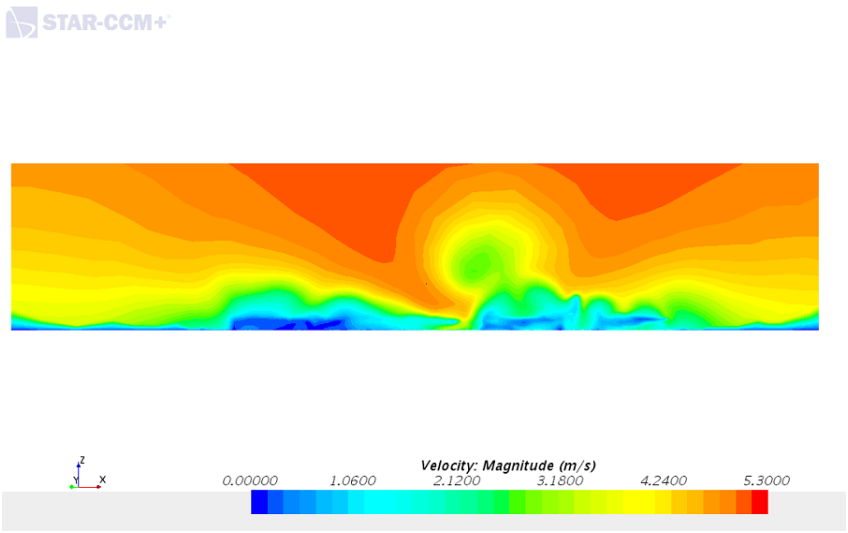

(a)

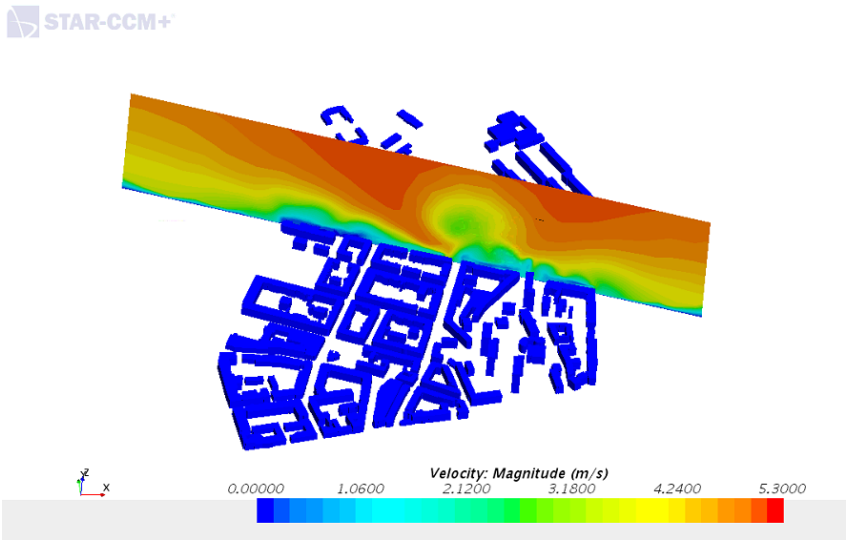

(b)

Figure 4.25: **(a)** The velocity shown in section X2 in Region 3 **(b)** The location of section X2 shown in the first image

Figure 4.24 and 4.25 shows the two sections normal to the flow direction in region 3. The two sections is placed in two streets. The hole in view in figure 4.24 is due to the fact the section is cutting in to a building.

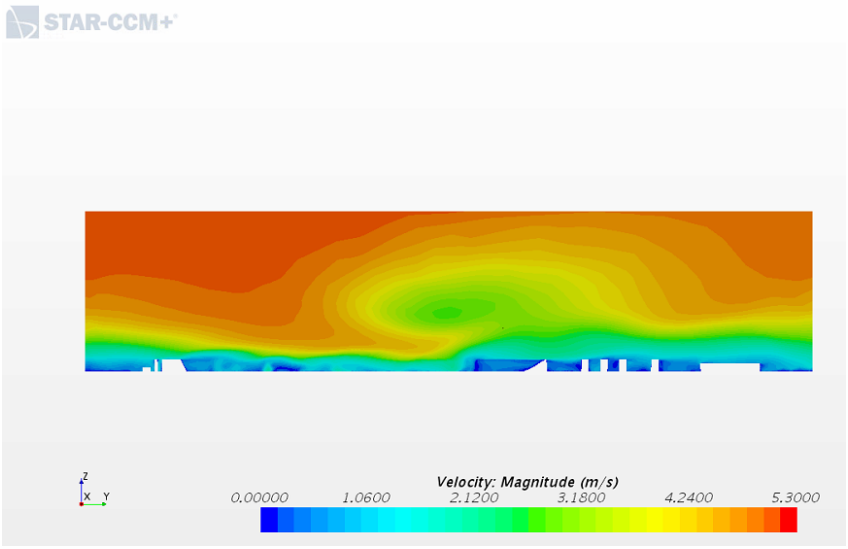

(a)

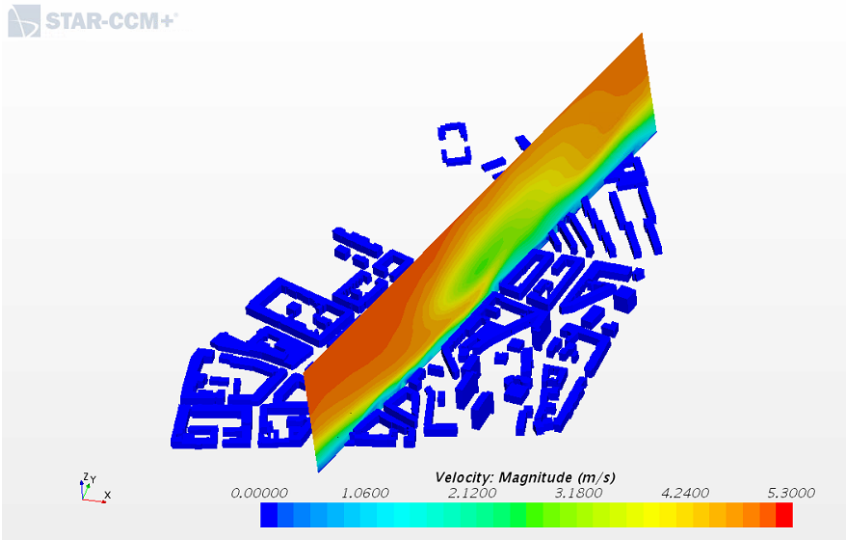

(b)

Figure 4.26: **(a)** The velocity shown in section Y1 in Region 3 **(b)** The location of section Y1 shown in the first image

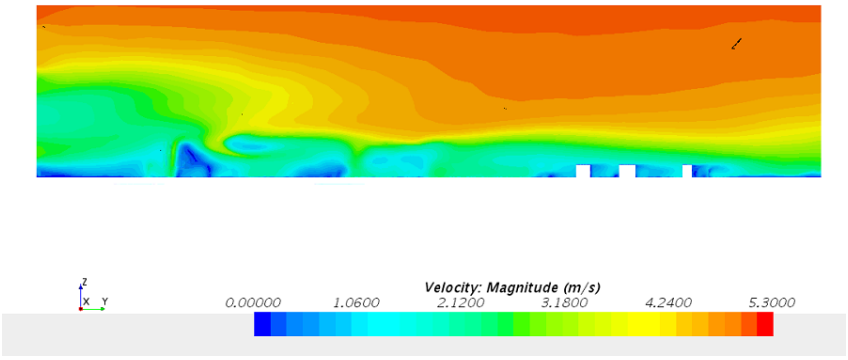

(a)

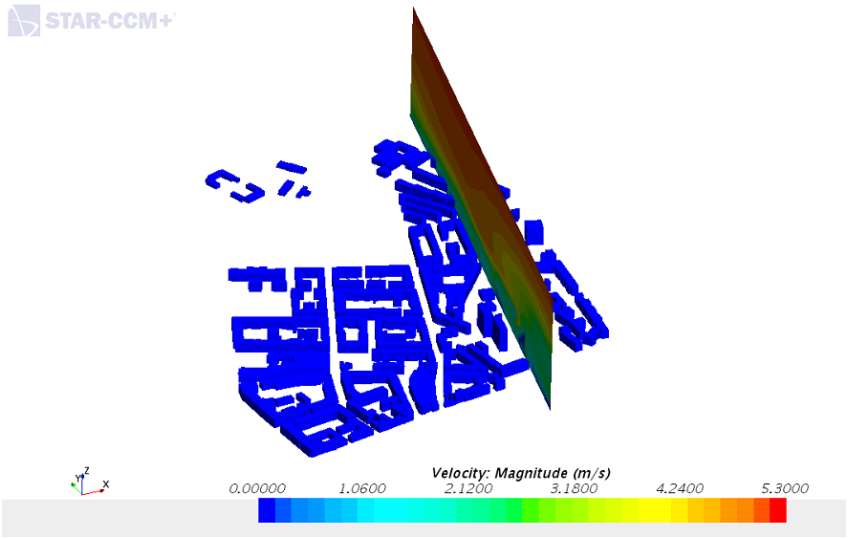

(b)

Figure 4.27: **(a)** The velocity shown in section Y2 in Region 3 **(b)** The location of section Y2 shown in the first image

Figure 4.26 and 4.27 shows to canyons in region 3 along the flow direction. Both sections are place in a street to see the velocity magnitude in these canyons.

4.4 Region 4

The last part of region 3 is a park with a lot of open space, the park is also a part of region 4. This means that the region is very open and the buildings do not have a lot of cover from the previous region.

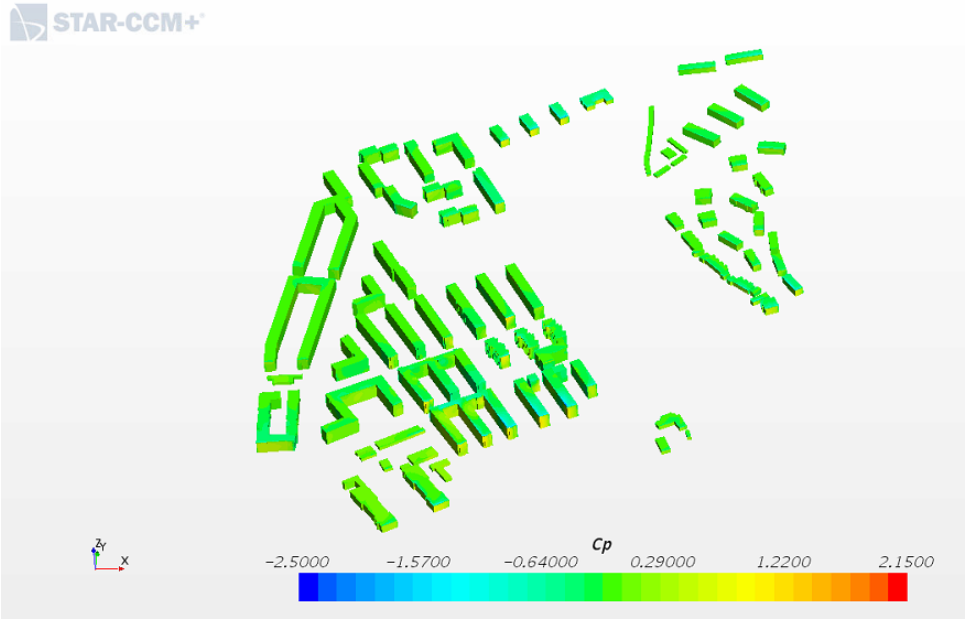

Figure 4.28: Pressure coefficients in Region 4

Figure 4.28 shows the pressure coefficients in region 4. The region is dominated by having a park, and therefore being quite open. This shows by the high Cp values in front of the region and also the exposed buildings in the back. The buildings on the left are taller than the buildings on the right. This means a bigger surface for the wind, and the pressure coefficients are higher on the buildings on the left side of the region.

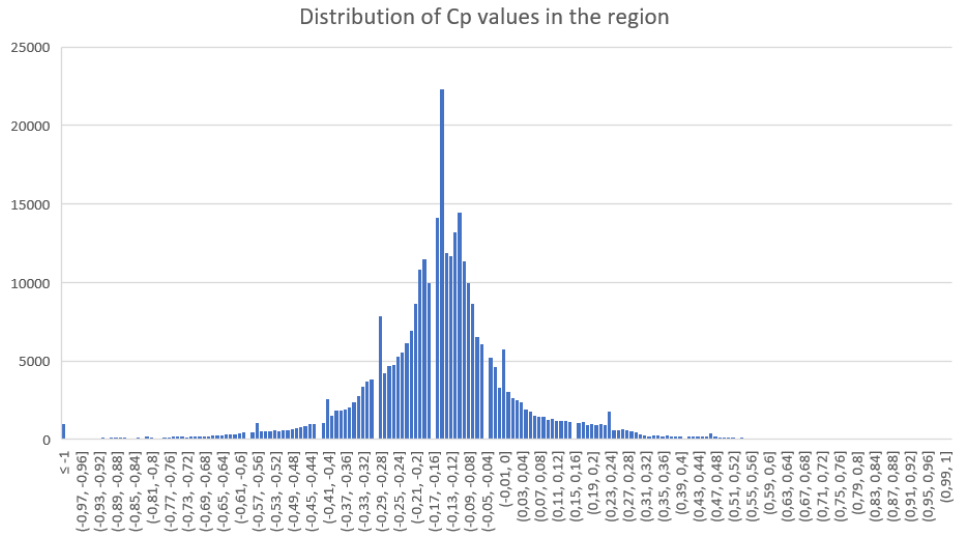

Figure 4.29: Distribution of the Pressure coefficients in Region 4

The Cp values varies more in this region than in the previous, the highest Cp value is 1.25 and the lowest is -2.8. The average Cp value in region 4 is -0.144. The distribution of the pressure coefficients in the region is shown in figure 4.30. The majority of points lies between -0.4 and 0.1.

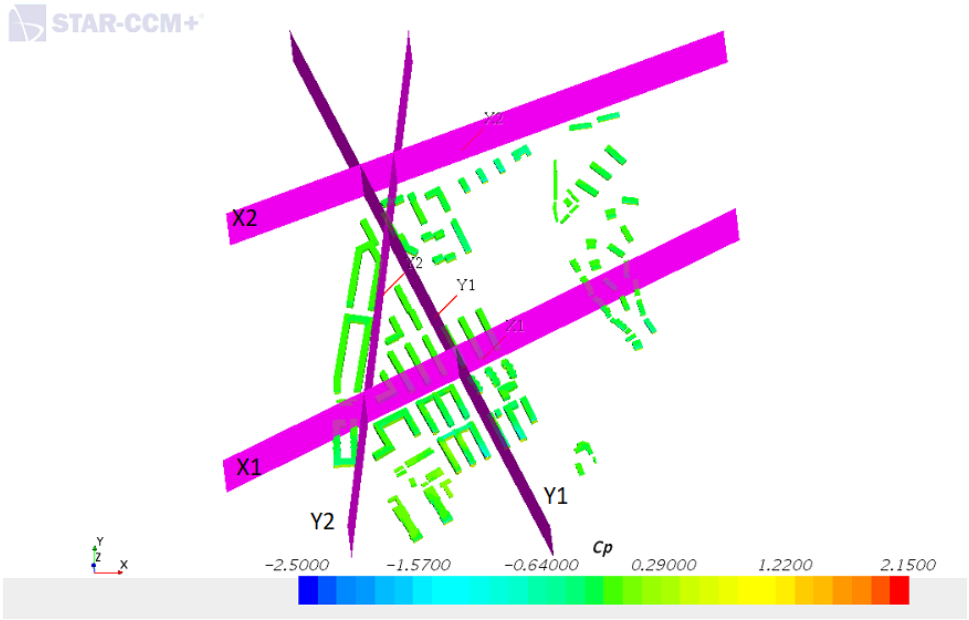

Figure 4.30: The location of the sections in Region 4

Figure 4.30 shows the four sections location in region 4. Section X1 and X2 is placed normal to the flow direction, both ranges from the left side if the region where there is taller buildings to the right side where there are low-rise buildings. X1 is placed in a

street and X2 is placed behind the last row of buildings in the region. The two sections Y1 and Y2 is placed in two streets as shown in figure 4.30.

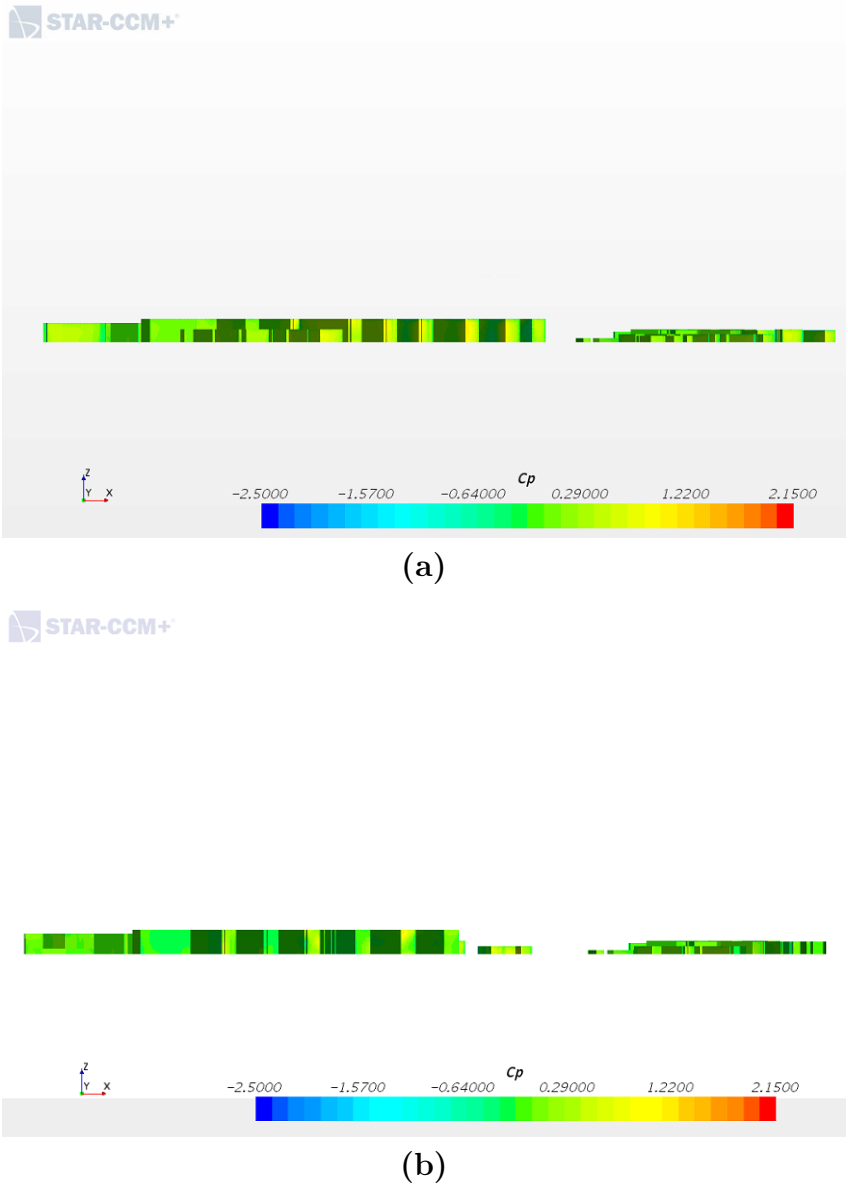

Figure 4.31: **(a)** The pressure coefficients in the front line of Region 4 **(b)** The pressure coefficients in section X1 in Region 4

Figure 4.31 shows the pressure coefficients in two views normal to the flow direction in region 4. Image a) is the front line of the buildings in the region, and image b) is view from section X1 in 4.30.

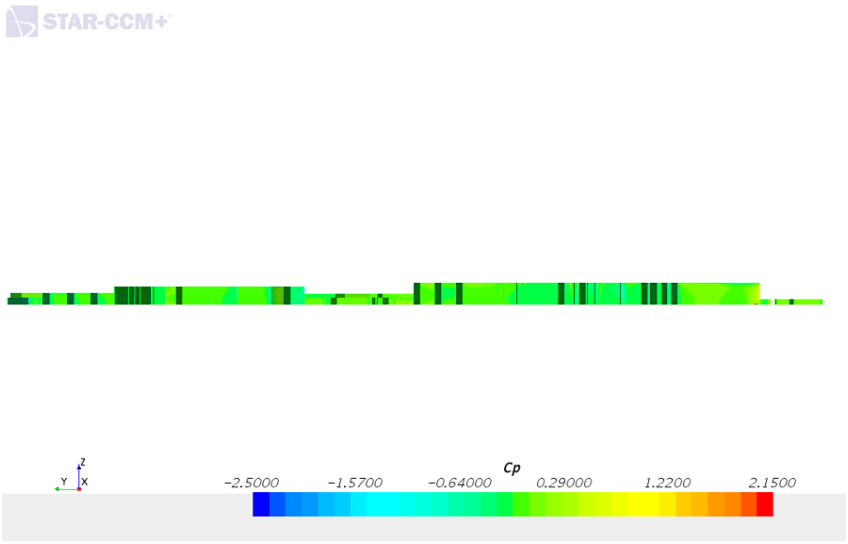

(a)

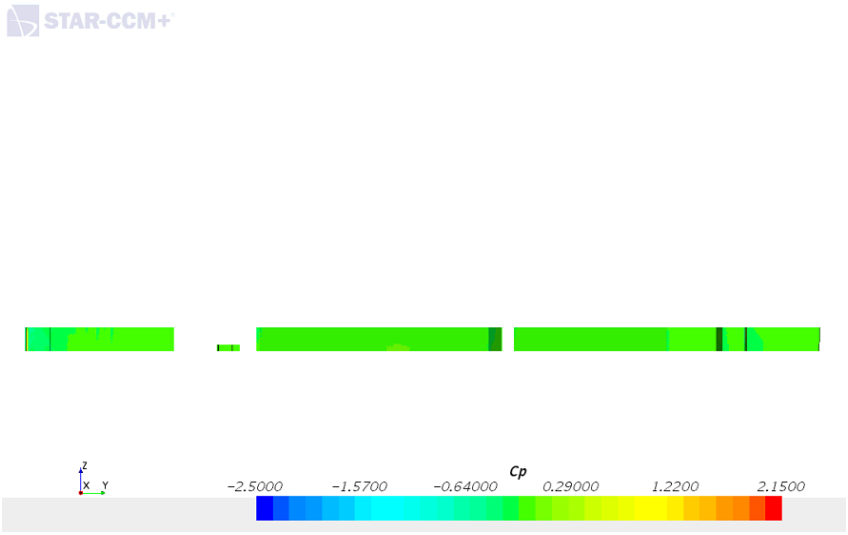

(b)

Figure 4.32: **(a)** The pressure coefficients in section Y1 in Region 4 **(b)** The pressure coefficients in section Y2 in Region 4

The pressure coefficients along the flow direction is shown in figure 4.32. Image a) is the left side of the region with the flow direction to the left. Image b) is the view from section Y2 in figure 4.30 with the flow direction to the right.

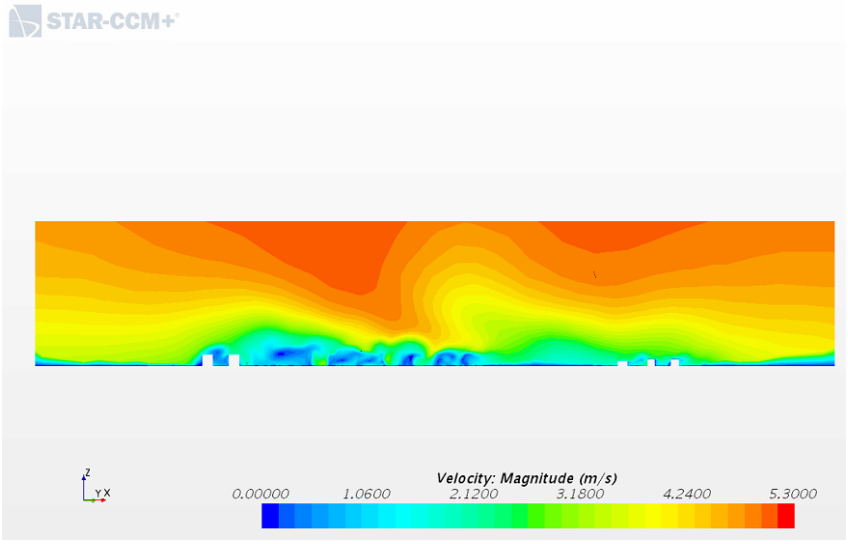

(a)

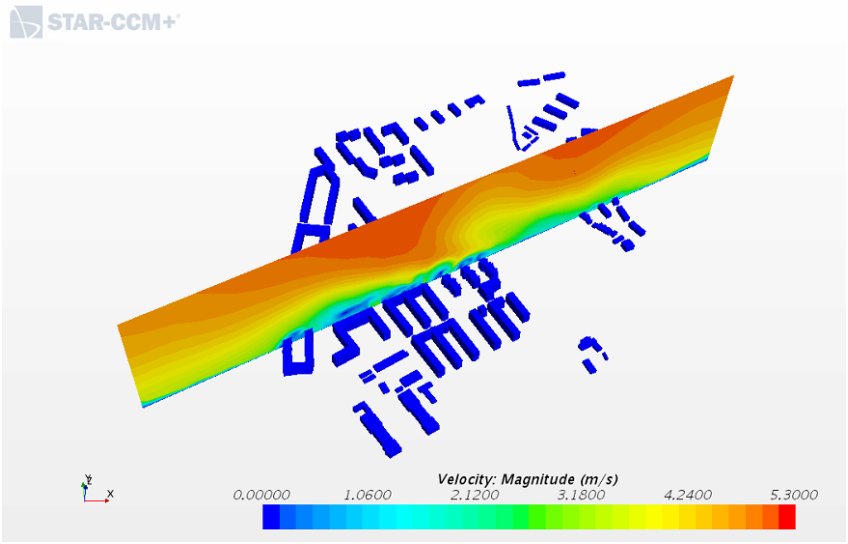

(b)

Figure 4.33: **(a)** The velocity shown in section X1 in Region 4 **(b)** The location of section X1 shown in the first image

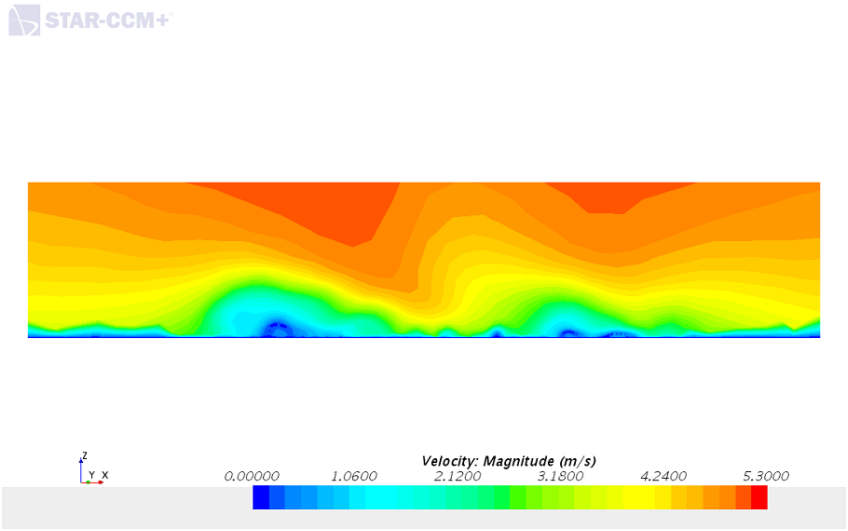

(a)

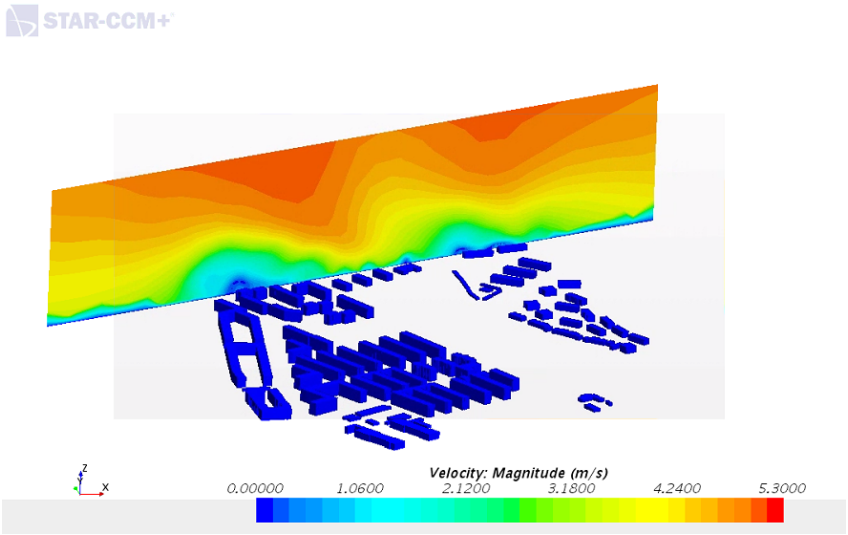

(b)

Figure 4.34: **(a)** The velocity shown in section X2 in Region 4 **(b)** The location of section X2 shown in the first image

Figure 4.33 and 4.34 shows two sections normal to the flow direction. Section X1 is placed in a street where both the low-rise buildings and the taller buildings is represented and X2 is a section directly behind the last row of buildings in the region.

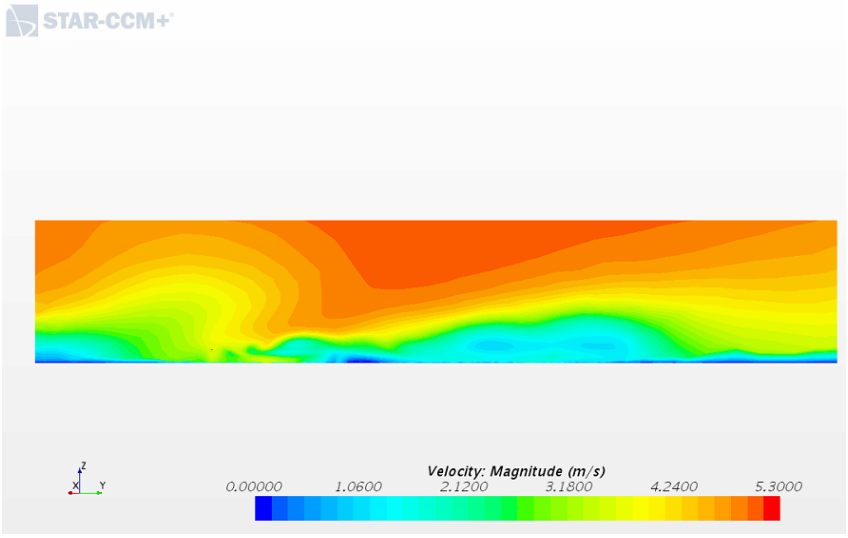

(a)

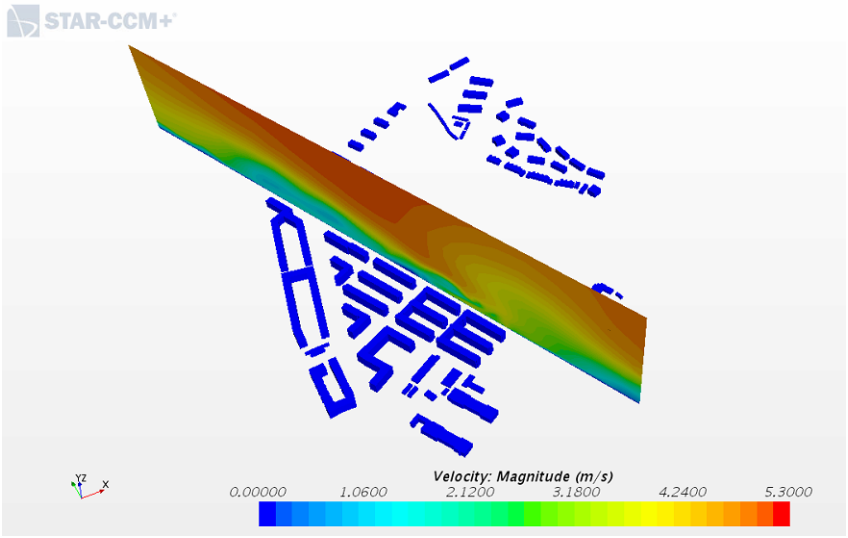

(b)

Figure 4.35: **(a)** The velocity shown in section Y1 in Region 4 **(b)** The location of section Y1 shown in the first image

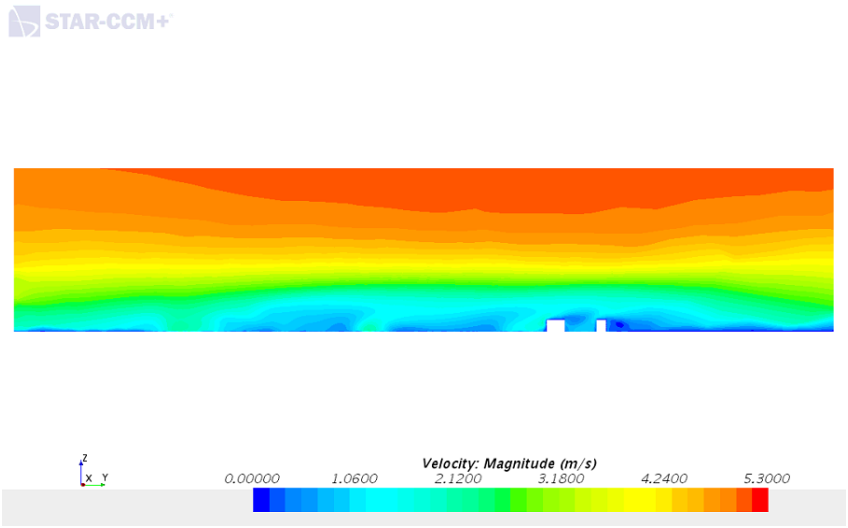

(a)

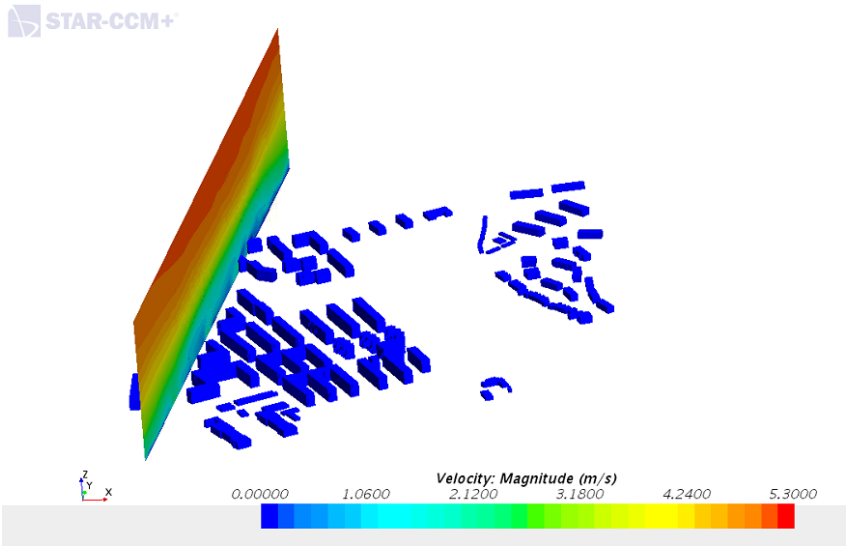

(b)

Figure 4.36: **(a)** The velocity shown in section Y2 in Region 4 **(b)** The location of section Y2 shown in the first image

Figure 4.35 and 4.36 shows to canyons along the flow direction in region 4. Both section is along two streets in the part of the region with taller buildings.

4.5 Region 5

The fifth region has a different set up than the rest, the inlet surface has an angle as shown in figure 3.9. The region has mostly low-rise buildings with some exceptions in the start of the region, this is also where the Cp values are highest.

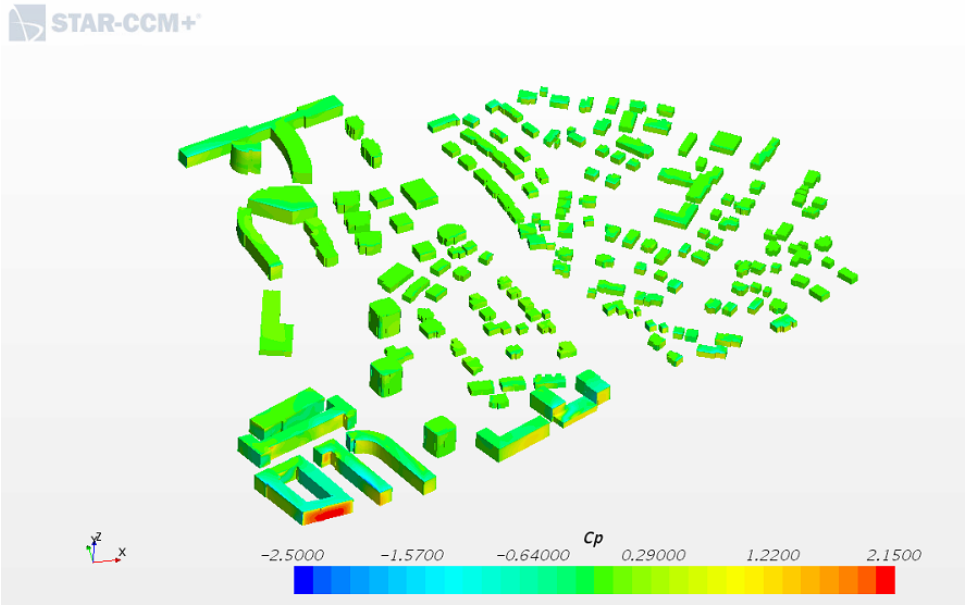

Figure 4.37: Pressure coefficients in Region 5

Figure 4.37 shows the pressure coefficients in region 5. The region mostly consist of low-rise buildings with a portion of taller buildings on the left side of the region. The previous region provides little cover against the wind and this shows on the building facades on the front line of this region, where the values are higher than the rest of the region. Particularly the building facade on the left is exposed to the wind because it has no cover from the previous region.

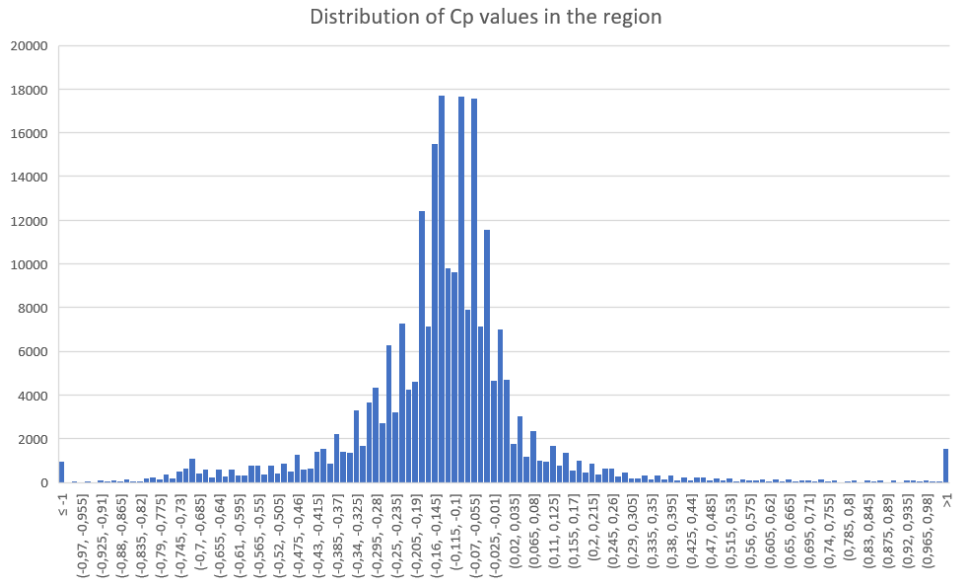

Figure 4.38: Distribution of the Pressure coefficients in Region 5

The Cp values in region 5 varies from the highest value at 2.1 to the lowest value at -2.6. The average Cp number is -0.127.

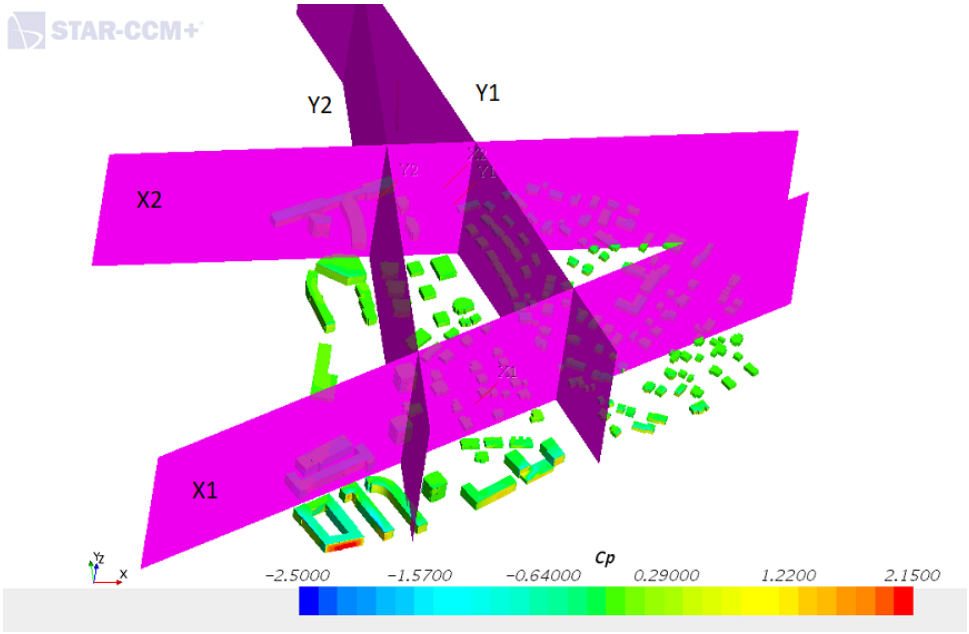

Figure 4.39: The location of the sections in Region 5

Figure 4.39 shows the four sections in region 5. Section X1 and X2 is normal to the flow direction and section Y1 and Y2 is along the flow direction. Region 5 has low-rise buildings and taller buildings, and the sections X1 and X2 aims to inlude both of these areas.

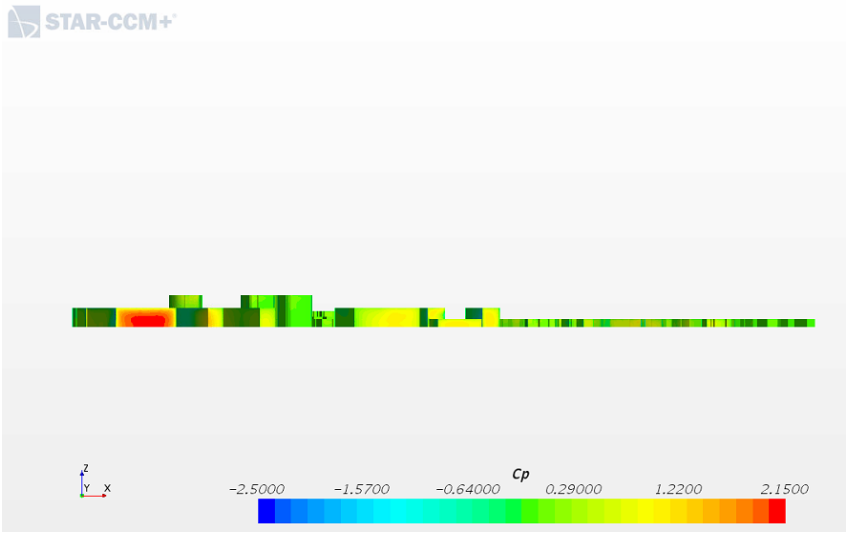

(a)

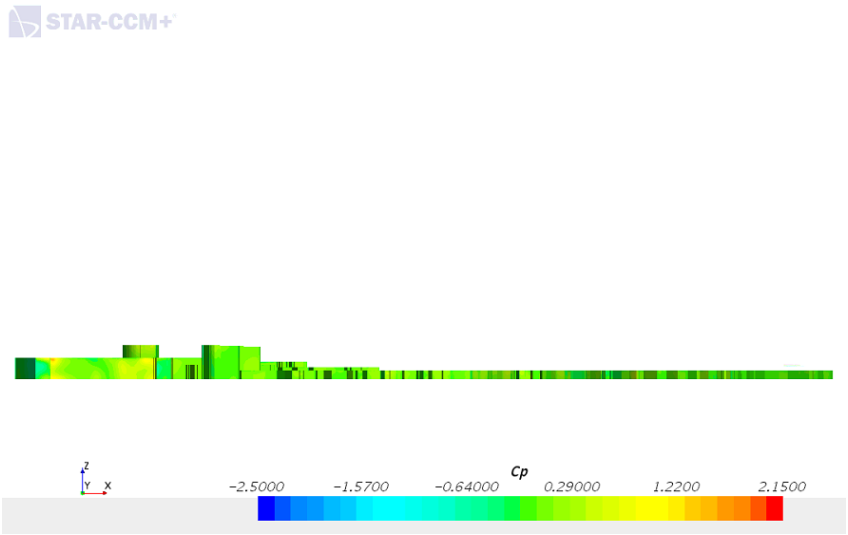

(b)

Figure 4.40: **(a)** The pressure coefficients in the front of Region 5 **(b)** The pressure coefficients in section X1 in Region 5

Figure 4.40 two views normal to the flow direction in region 5 is shown. Image a) shows the pressure coefficients in the front line of region 5, image b) shows the view from section X1 in figure 4.39. From image a) it is clear that the building on the left is exposed and not getting cover from the previous region. Image b) is deeper in the region and is more covered.

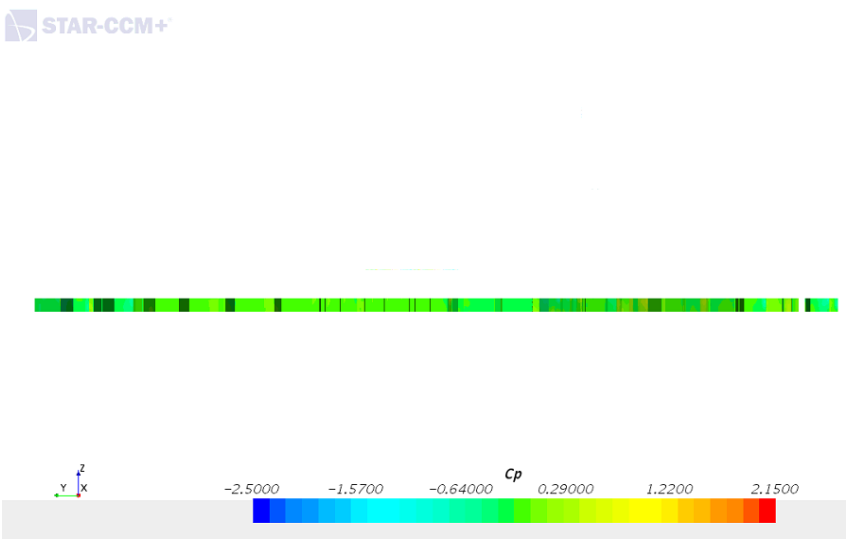

(a)

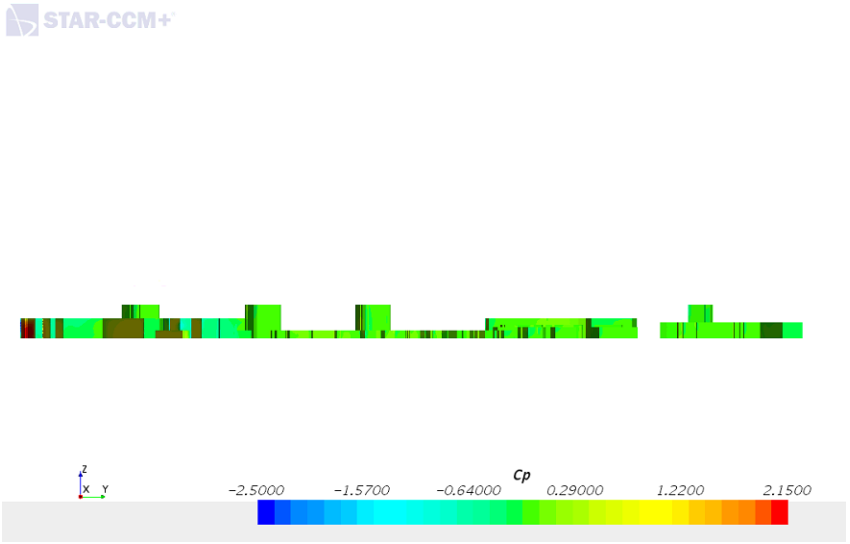

(b)

Figure 4.41: **(a)** The pressure coefficients in section Y1 in Region 5, flow direction to the left **(b)** The pressure coefficients in section Y1 in Region 5, flow direction to the right

The pressure coefficients in two views along the flow direction is shown in figure 4.41. Image a) and image b) is from the same section, section Y1 from figure 4.39. However the views are directed in opposite angles, image a) with the flow direction to the left and image b) to the right.

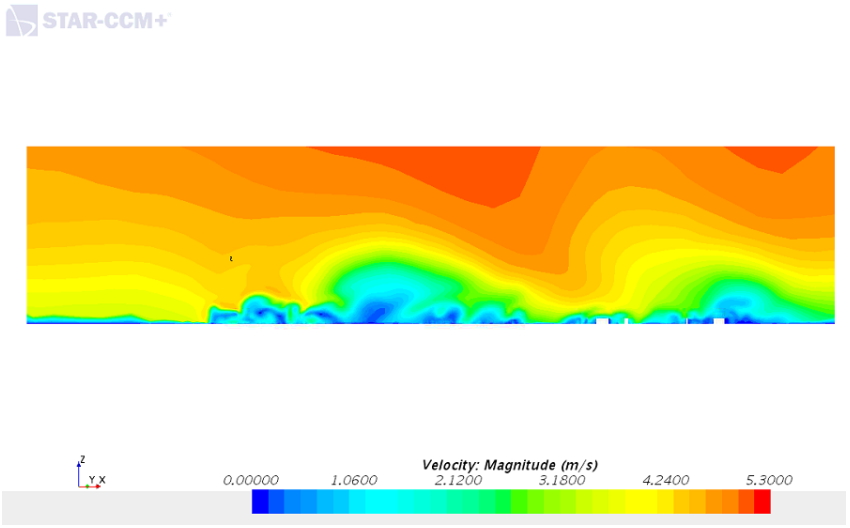

(a)

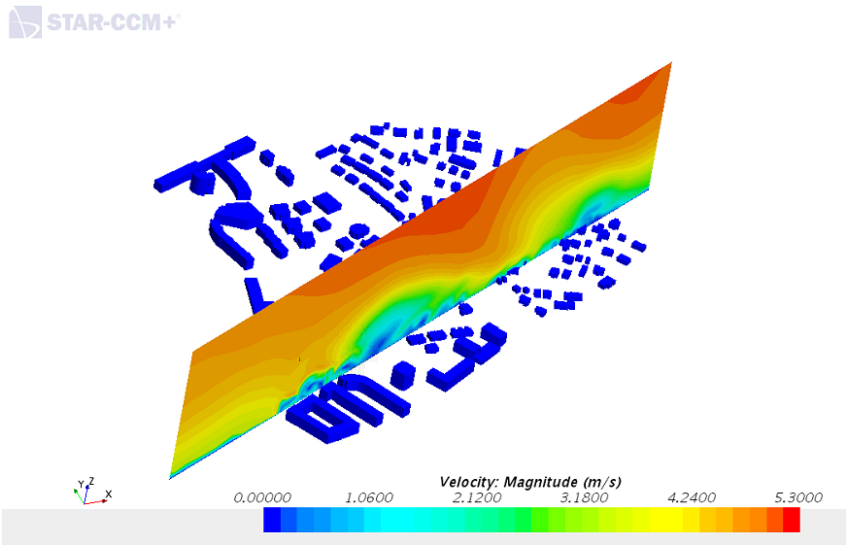

(b)

Figure 4.42: **(a)** The velocity shown in section X1 in Region 5 **(b)** The location of section X1 shown in the first image

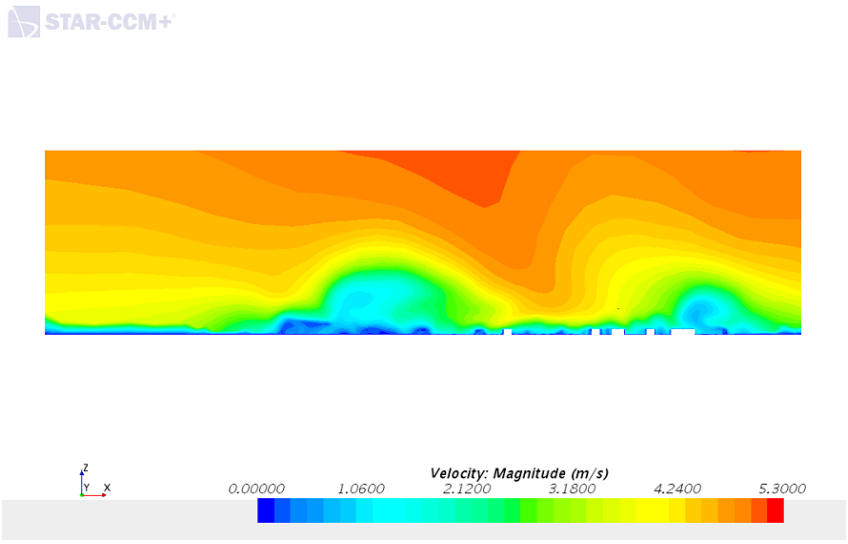

(a)

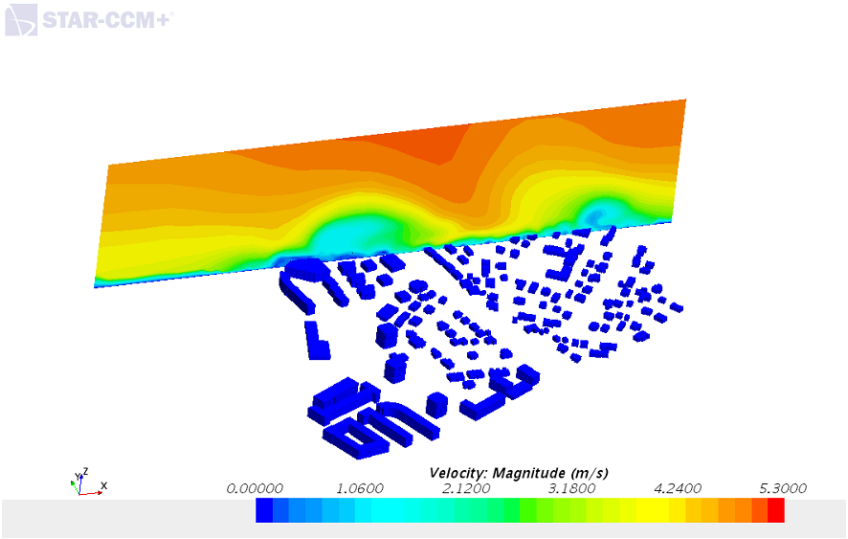

(b)

Figure 4.43: **(a)** The velocity shown in section X2 in Region 5 **(b)** The location of section X2 shown in the first image

The two sections normal to the flow direction is shown in figure 4.42 and 4.43. The velocity magnitude is shown in to sections, section X1 is located at the front part of the region and X2 is placed at the back part of the region.

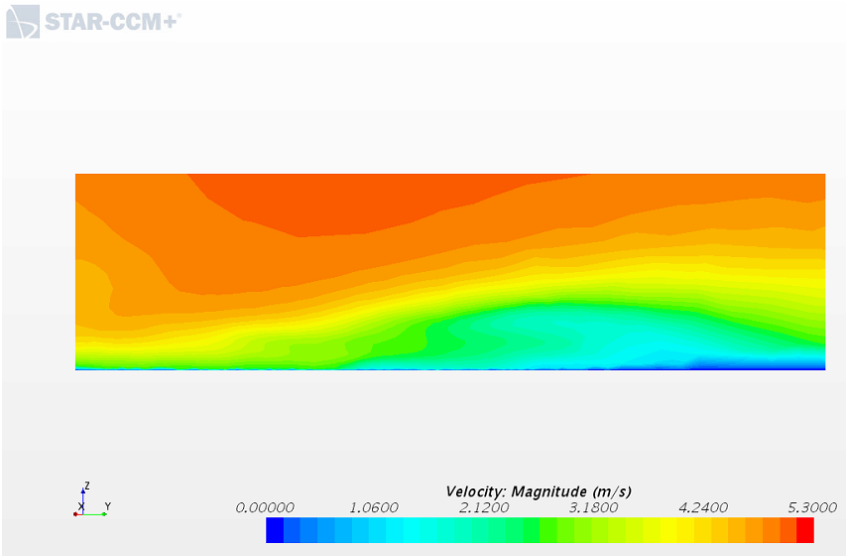

(a)

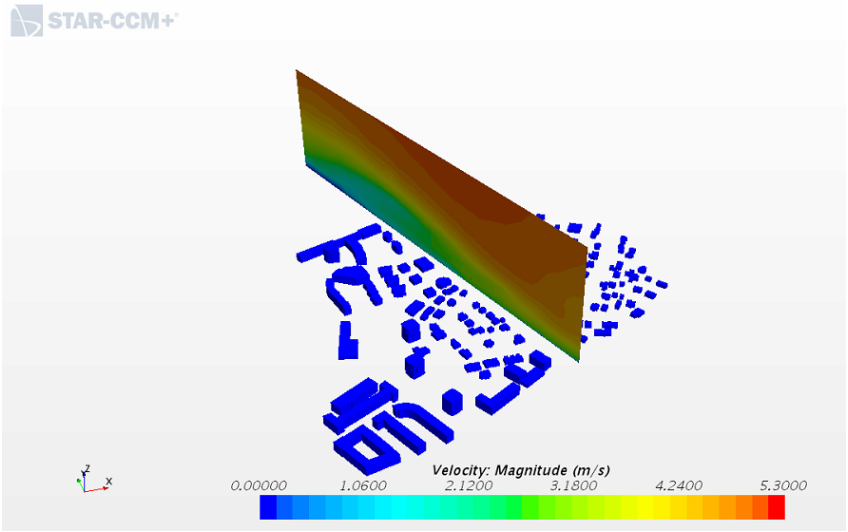

(b)

Figure 4.44: **(a)** The velocity shown in section Y1 in Region 5 **(b)** The location of section Y1 shown in the first image

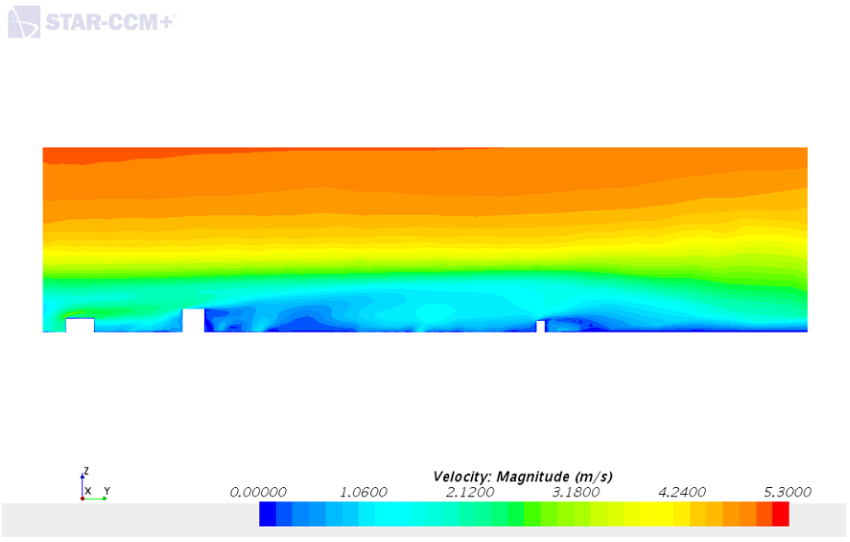

(a)

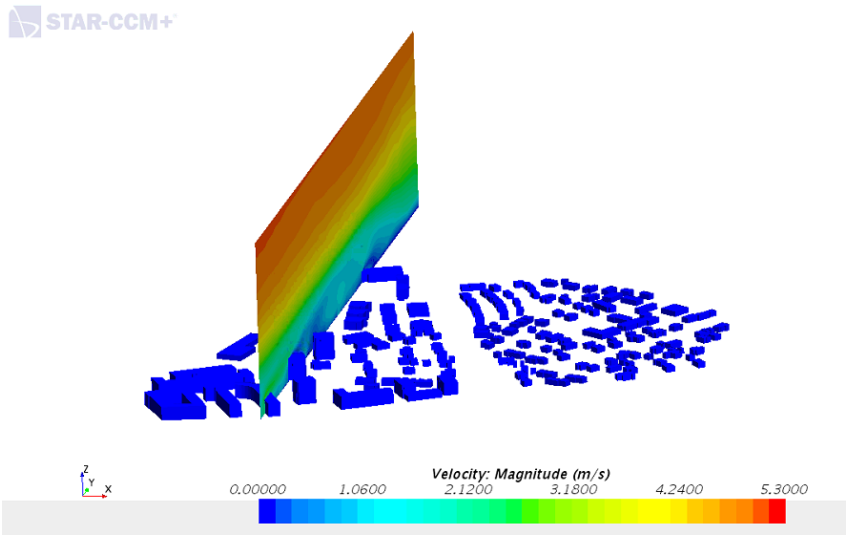

(b)

Figure 4.45: **(a)** The velocity shown in section Y2 in Region 5 **(b)** The location of section Y2 shown in the first image

Figure 4.44 and 4.45 shows two sections where the plane is along the flow direction. Y1 is located in the canyon between the low-rise buildings and the taller buildings. Y2 is located in a more diagonal street on the left side of the region.

5 Discussion

The five different regions varies in terms of aspect ratio and in terms of relations between the regions. For example between region 1 and 2 there is a considerable amount of open space due to the railway, however between region 2 and 3 the amount of open space is very little. This does have an effect on the pressure coefficients in the regions.

An aspect of the study that turned out to be a significant part of the study was the workflow of the file formats. To achieve import of the original SOSI file was challenging, and is something that was time consuming. The option to model the geometry either in Star CCM+ or any other 3D modelling program was there, but was not really considered in order to get the authenticity of the actual geometry of the city of Oslo.

5.1 Pressure coefficients

The pressure coefficients are highest on the building facades facing the wind direction, and the buildings that are exposed by having an open space in front of them. The negative pressure coefficients occurs on the sides of the facades that has a high pressure coefficient value.

In region 1 the distribution of pressure coefficients varies a lot, this is because the region is dominated by high-rise buildings and they are completely exposed to the wind from the sea. On the other hand in region 3, where the buildings are lower and denser the pressure coefficients varies much less. It is clear that what governs the high pressure coefficient values is in what degree the building facade is exposed to the wind. If the facade is placed normal to the flow direction and with little cover in front, the values will be high with negative values on the sides. That again indicates that the location of the negative pressure coefficients is found on the sides of the facades that have a high pressure coefficient value. This is also clear from looking at region 5 where most of the geometry is well covered by the previous region with the exception of the building on the outskirt of the region, where the pressure coefficients are much higher than the rest of the region. This is due to the wind exposure and lack of cover from the previous region.

5.2 Wind velocity

It is a known phenomenon that wind tends to be a problem around high-rise buildings and this can be a problem for pedestrian comfort. In streets around high-rise buildings the wind tends to accelerate around corners and on pedestrian levels. This can be seen on the X and Y sections of region 1, where the buildings are tall. The wind velocity is high around the buildings, this can be seen in figure 4.9. Also from the figure 4.4 it is clear that the velocity picks up in the canyon between the buildings. When the buildings becomes lower, like region 3 where the number of high-rise buildings is reduced the velocity is not that high around the buildings. However, there are some turbulence around the high-rise buildings seen in figure 4.24. This indicates that when there are a few much higher buildings than the norm in the region this will affect the wind conditions.

6 Conclusion

In this study, Star CCM+ has been used as a CFD tool in order to simulate and chart the wind velocity and the pressure coefficients in five regions Oslo. The Pressure coefficients in a region is dependent on the aspect ratio of buildings and street, but also dependant on the relation with the previous region. The Cp values are typically highest on the building facades which is facing the wind direction. The negative pressure coefficients occurs on the sides of the facades that has a high pressure coefficient value. Region 1 has high pressure coefficients values on the first row of buildings because they are exposed to the seaside, the same can be observed in region 2 where the railway ensures an open space before region 2. When it comes to the wind velocity in the regions, the aspect ratio does make an impact. When the wind hits normal to a street canyon it creates a wind vortex on the leeward side and increased velocities in the canyon.

The pressure distribution in the regions varied quite a lot. The region 1, where the buildings were most exposed to the wind had the most varying distribution of the five regions. This shows that one will achieve varying pressure coefficients in a region that is exposed to wind from the sea, like it is in Oslo, Barcode. Four of five regions shows a negative average pressure coefficient value, the region that has the highest average is region 3. Not only the highest, but it is also the only region with a positive average pressure coefficient. This is due to the region being the larges and the most dense. This leads to the buildings being the least exposed and the values varies much less as a result.

References

Abubaker, A., Kostić, I., and Kostić, O. (2018). Numerical modelling of velocity profile parameters of the atmospheric boundary layer simulated in wind tunnels. In *IOP Conference Series: Materials Science and Engineering*, volume 393, page 012025. IOP Publishing.

Blocken, B. and Carmeliet, J. (2004). Pedestrian wind environment around buildings: Literature review and practical examples. *Journal of Thermal Envelope and Building Science*, 28(2):107–159.

Blocken, B., Stathopoulos, T., and Carmeliet, J. (2007). Cfd simulation of the atmospheric boundary layer: wall function problems. *Atmospheric environment*, 41(2):238–252.

Blocken, B., Stathopoulos, T., and Van Beeck, J. (2016). Pedestrian-level wind conditions around buildings: Review of wind-tunnel and cfd techniques and their accuracy for wind comfort assessment. *Building and Environment*, 100:50–81.

Bottema, M. (1993). Wind climate and urban geometry.

Bottema, M. (2000). A method for optimisation of wind discomfort criteria. *Building and Environment*, 35(1):1–18.

Clayton, R. (2019). Wind loading for architectural glazing.

Cóstola, D., Blocken, B., Ohba, M., and Hensen, J. (2010). Uncertainty in airflow rate calculations due to the use of surface-averaged pressure coefficients. *Energy and Buildings*, 42(6):881–888.

Dagnew, A. and Bitsuamlak, G. T. (2013). Computational evaluation of wind loads on buildings: a review. *Wind Struct*, 16(6):629–660.

Grimenes, A. and Thue-Hansen, V. (2004). Annual variation of surface roughness obtained from wind profile measurements. *Theoretical and applied climatology*, 79(1-2):93–102.

He, J. and Song, C. C. (1999). Evaluation of pedestrian winds in urban area by numerical approach. *Journal of Wind Engineering and Industrial Aerodynamics*, 81(1-3):295–309.

Holmes, J. D. (2018). *Wind loading of structures*. CRC press.

Jurelionis, A. and Bouris, D. G. (2016). Impact of urban morphology on infiltration-induced building energy consumption. *Energies*, 9(3):177.

Krishna, P. (1995). Wind loads on low rise buildings—a review. *Journal of wind engineering and industrial aerodynamics*, 54:383–396.

Lawson, T. and Penwarden, A. (1977). The effects of wind on people in the vicinity of buildings.

Liu, S., Pan, W., Zhang, H., Cheng, X., Long, Z., and Chen, Q. (2017). Cfd simulations of wind distribution in an urban community with a full-scale geometrical model. *Building and Environment*, 117:11–23.

Murakami, S., Uehara, K., and Deguchi, K. (1980). Wind effects on pedestrians: New criteria based on outdoor observation of over 2000 persons. In *Wind Engineering*, pages 277–288. Elsevier.

of Japan (AIJ), A. I. (1996). *AIJ recommendations for loads on buildings*. Architectural Institute of Japan.

Parrish, D. D. and Zhu, T. (2009). Clean air for megacities. *Science*, 326(5953):674–675.

Simcenter (2020). MS Windows NT kernel description.

Srebric, J., Heidarinejad, M., and Liu, J. (2015). Building neighborhood emerging properties and their impacts on multi-scale modeling of building energy and airflows. *Building and Environment*, 91:246–262.

Tabrizi, A. B., Whale, J., Lyons, T., and Urmee, T. (2014). Performance and safety of rooftop wind turbines: Use of cfd to gain insight into inflow conditions. *Renewable Energy*, 67:242–251.

Versteeg, H. K. and Malalasekera, W. (2007). *An introduction to computational fluid dynamics: the finite volume method*. Pearson education.

Appendix

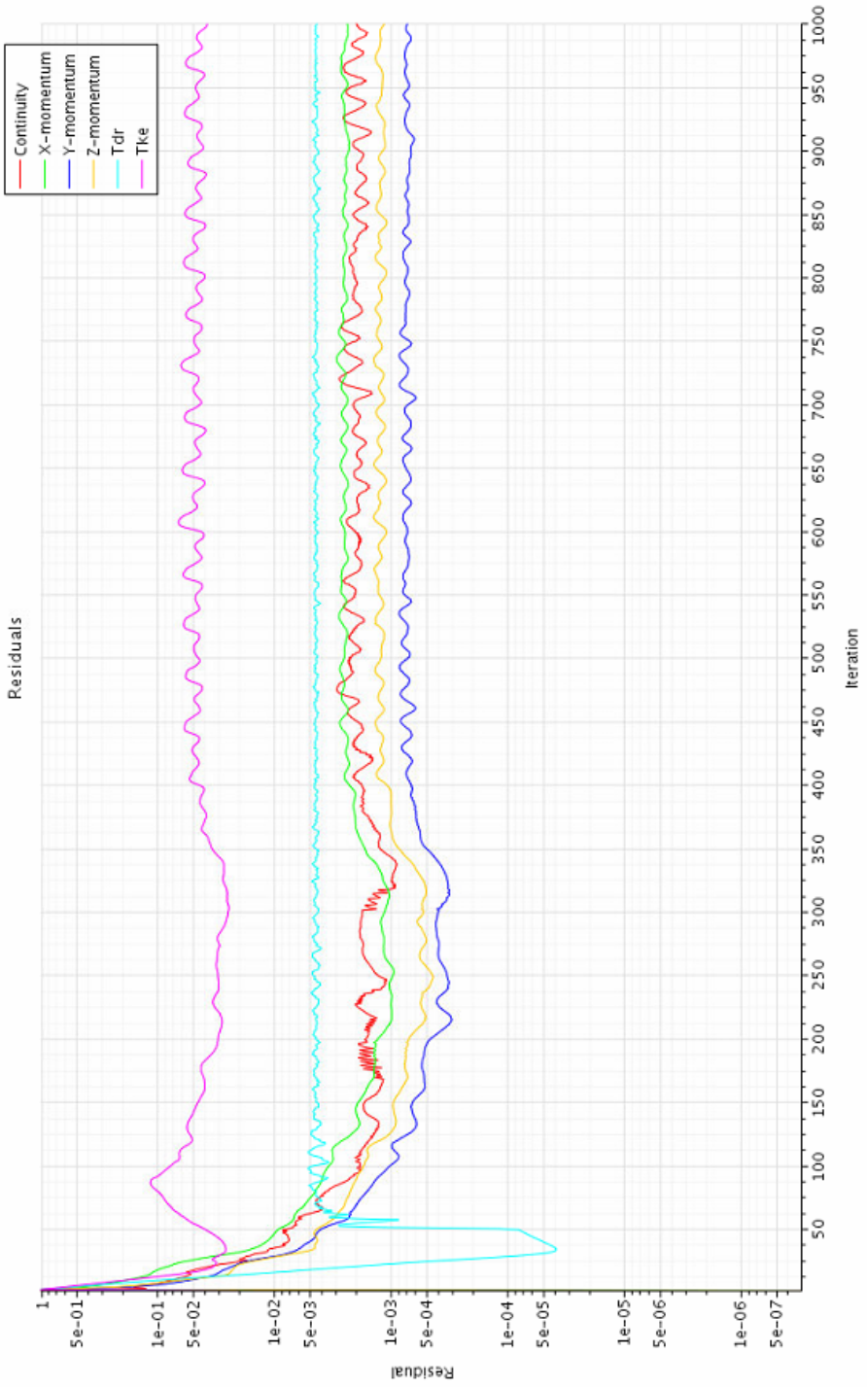

Figure A0.1: Residuals region 1

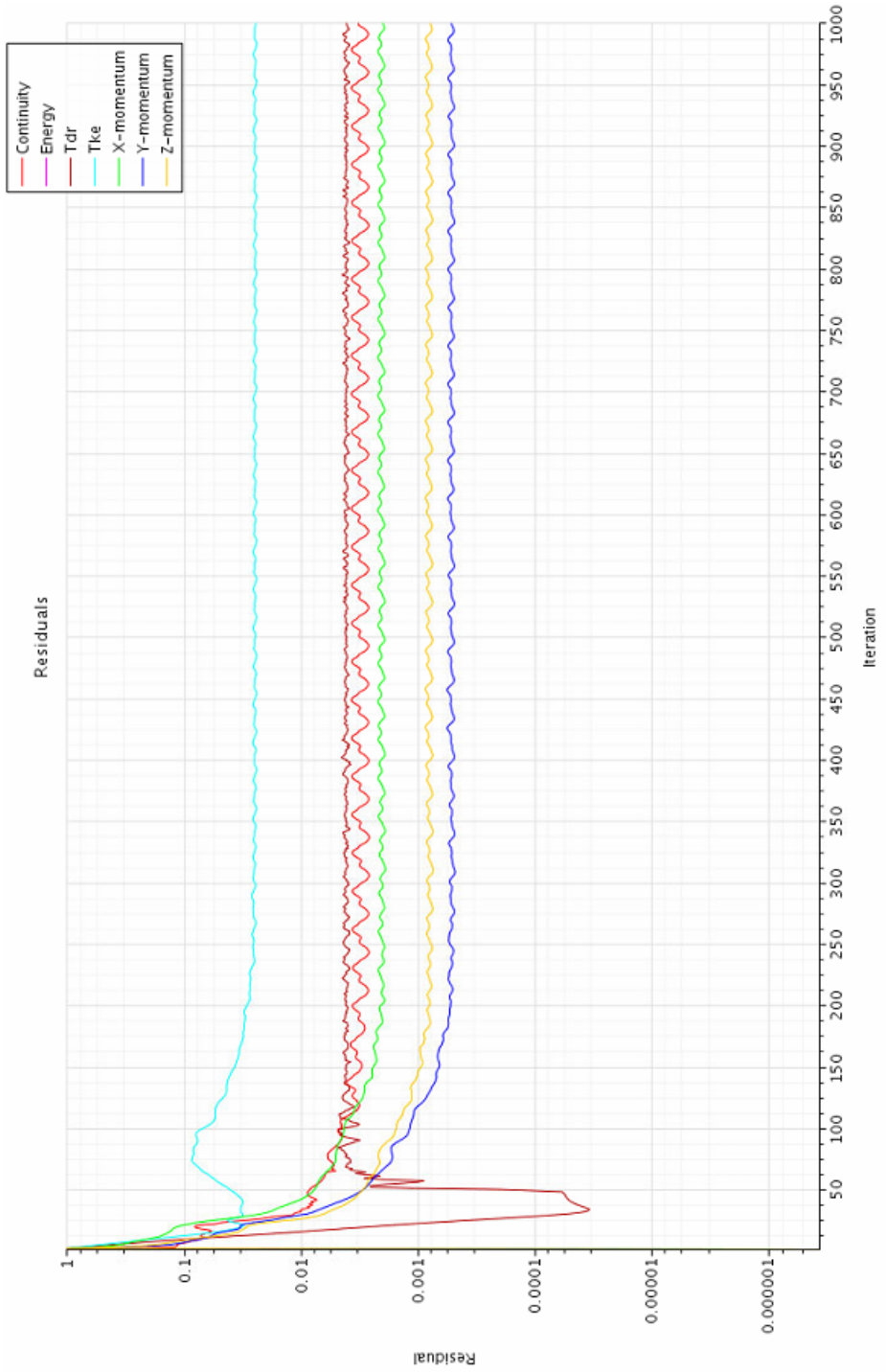

Figure A0.2: Residuals region 2

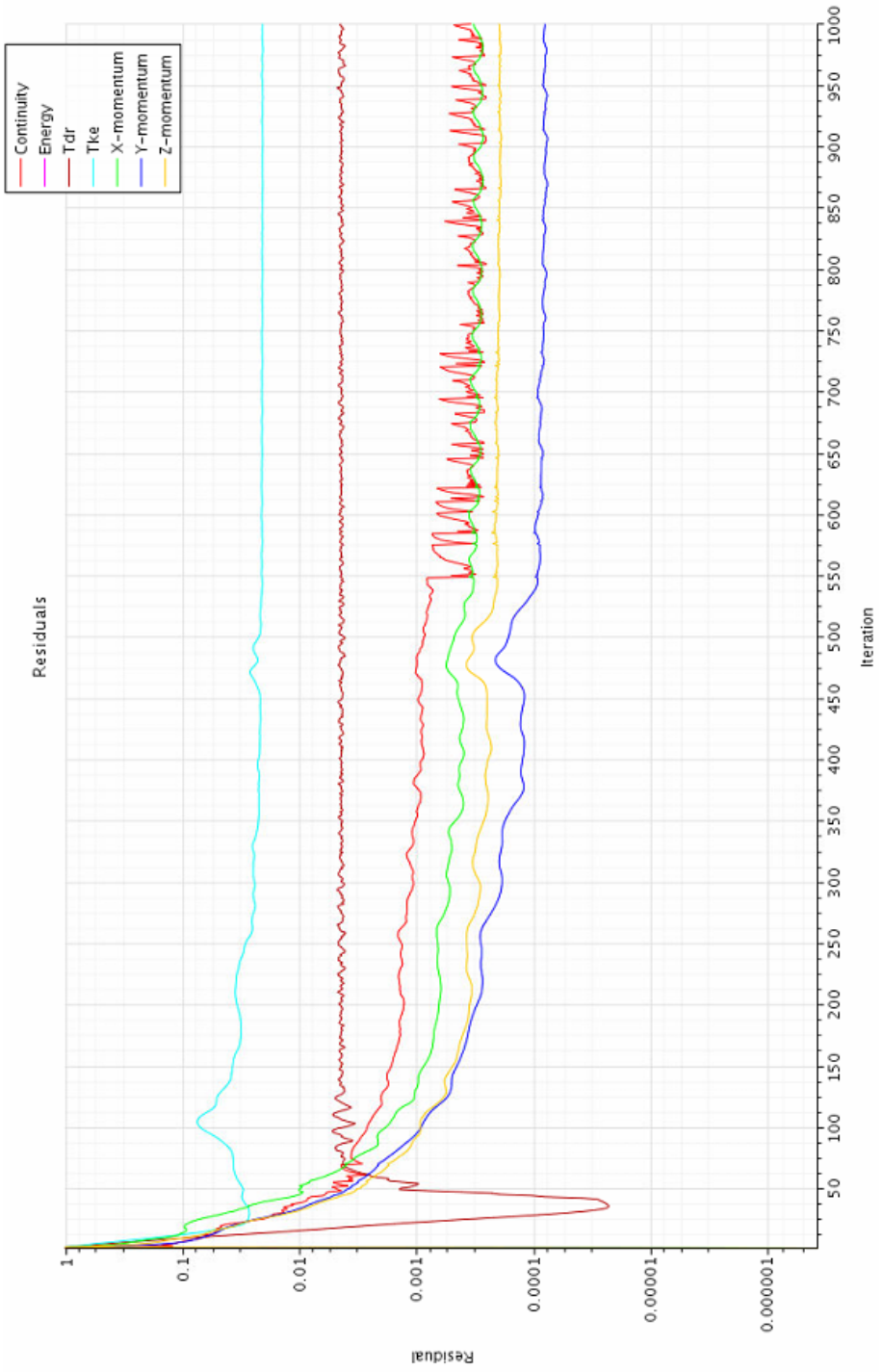

Figure A0.3: Residuals region 3

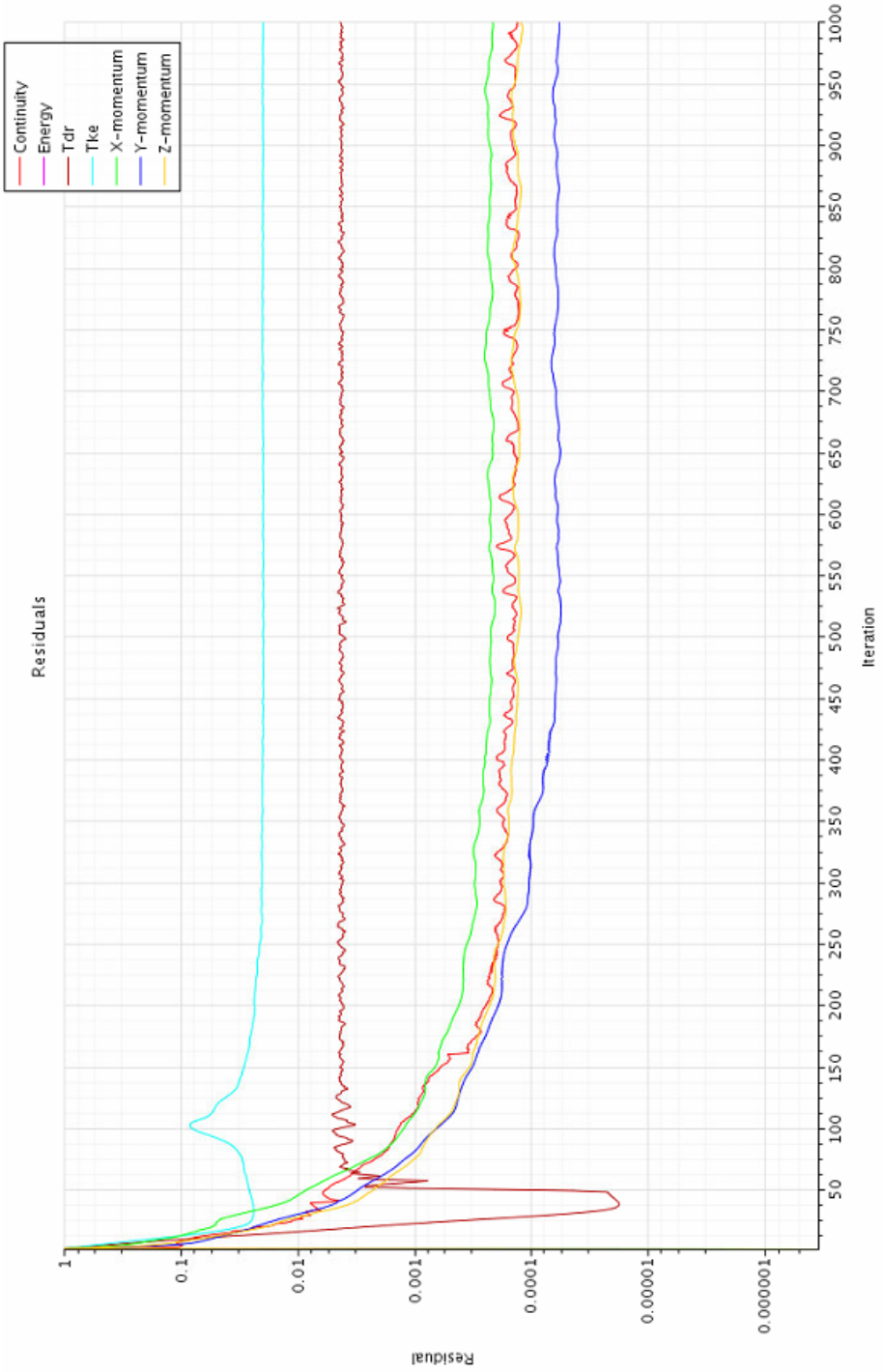

Figure A0.4: Residuals region 4

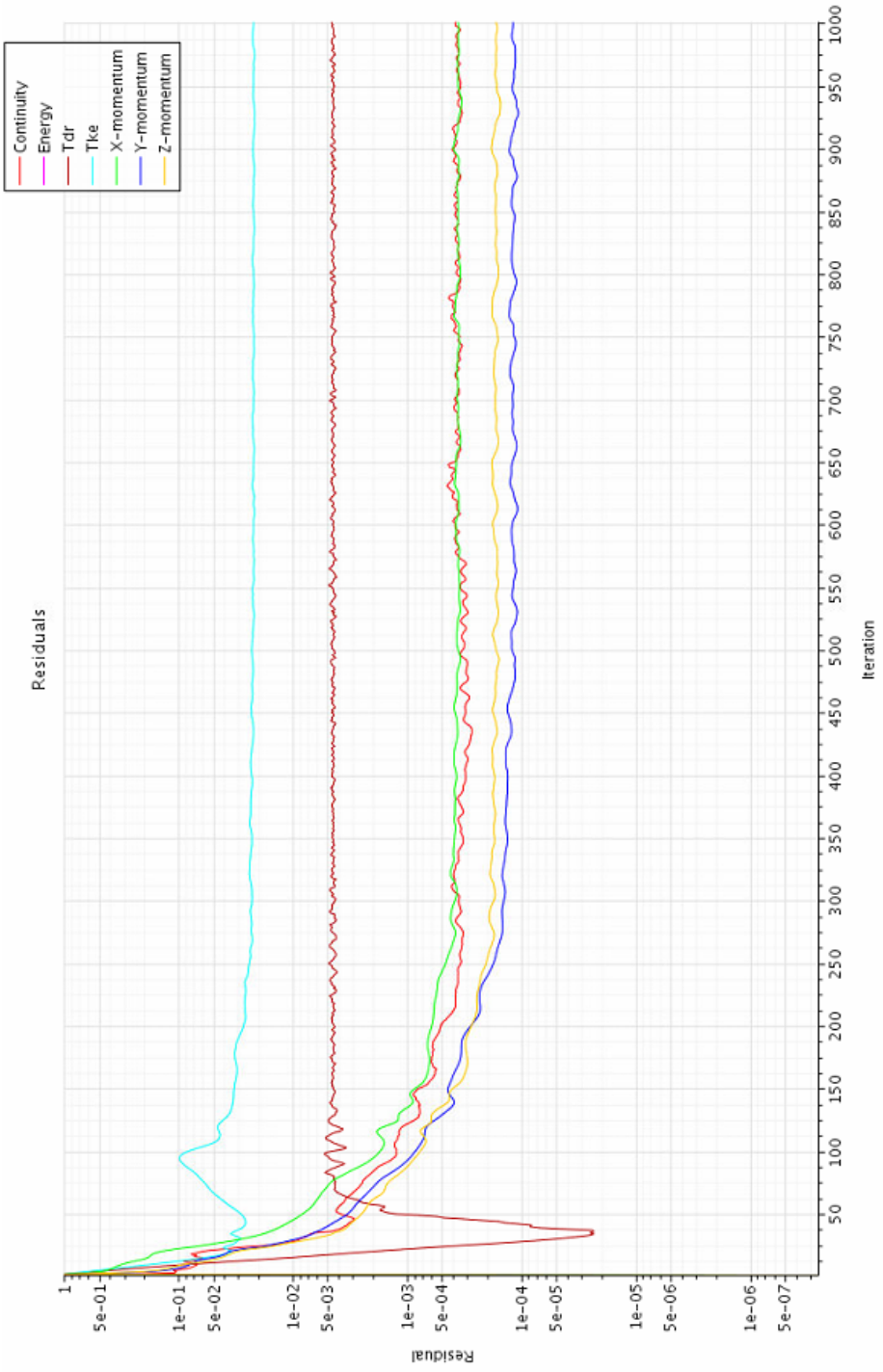

Figure A0.5: Residuals region 5